CAVITATION DETECTION IN A WATER JET PROPULSION UNIT

Hari Kallingalthodi

A thesis submitted in partial fulfilment of the requirements for the Degree of

Master of Engineering

in

Electrical and Computer Engineering

at the

University of Canterbury,

Christchurch, New Zealand

April 2009

Contents

Acknowledgements

I would like to thank my principal advisor Dr. Larry Brackney for his thoughtful guidance and generous support throughout this project. I am equally indebted to my co-supervisor Dick Borrett for his technical support and insightful suggestions during this project. It has been a privilege and pleasure to work with them.

I would also like to express my sincere appreciation to Mike Meade for his project advice, Ian Huntsman for technical suggestions, Rob Toshach for patiently helping me during tedious testing, Gordon Lissaman on instrumentation design and Peter Worley for his assistance in testing the sensors. Thanks also to all other members of Hamilton Jet technical team for being supportive during my time there and giving me the opportunity to be a part of their team.

Thanks are owing to Julian Murphy of Mechanical Engineering Dept. for his advice on instruments and Emily Hung for being very kind to me by translating a research paper despite her busy schedule.

Finally I would like to express gratitude to my family and friends for their affection and unbounded support they have given me throughout the years.

Abstract

Various sensing and digital signal processing approaches to detect cavitation in a water jet propulsion unit were examined based on results in the literature. Several commercially viable sensors were evaluated based upon their ability to detect the cavitation phenomenon, cost, and robustness. An algorithm has been implemented and tested against data recorded from the candidate sensors. The combination of vibration and pressure sensors and the algorithm appear promising and a path for further development and testing is available to Hamilton Jet.

List of Figures

1. Introduction

Cavitation is a term used to describe a process, which includes nucleation, growth and implosion of vapour or gas filled cavities. These cavities are formed when the static pressure of a liquid for one reason or another is reduced below the vapour pressure of the liquid at current temperature. Occurrence of cavitation is mostly detrimental to the hydraulic system. One of the harmful consequences of cavitation is mechanical damage to the solid materials of hydraulic system known as cavitation erosion.

Cavitation is a common phenomenon in all types of water jet units for marine propulsion. Cavitation erosion of water jet impellers and other mechanical parts is a major problem. Apart from that, it also reduces thrust of the jet and causes increased noise level and vibration. It is known that cavitation produces a distinct sound due to the violent implosion of cavitation bubbles. The implosion of bubbles on the mechanical surface causes vibration and shock waves through the mechanical structure.

The objective of this project is to develop an efficient, reliable, cost effective method to detect cavitation using low cost sensors and digital signal processing techniques that could be implemented in a real-time monitoring and control system. Implementing such a system would enable detection of cavitation at an early stage, allowing corrective action to reduce cavitation and thereby reducing the overall operational cost of water jets.

The rest of the report is organised as follows:

Chapter-2 gives a general description of cavitation phenomenon and the effects of cavitation on water jet. Chapter-3 devotes itself to a description and discussion of the state of the art in the field of cavitation detection and relevant patents in this field. Chapter-4 describes the sensors used in the experiment and instrumentation followed by the test procedures. Their specifications are also presented in this chapter. Chapter-5 presents the data analysis and the results obtained from the testing phase of the projects. Under separate sections, results from the rig tests and boat tests are also described. In chapter-6, the cavitation detection algorithm is presented. The implementation of the algorithm in Simulink and the simulation results are also described. Chapter-7 summarises the main results of the literature survey and key results of project. Conclusions are drawn from the results and recommendations are given for the continuation of the project. Finally, references and the detailed test plan of experiment done are also included at the end of this report.

This project was carried out at CWF Hamilton & Co. Ltd, Christchurch and the Electrical Engineering Department of the University of Canterbury.

2. Background to cavitation

Cavitation is the formation and activity of bubbles in a liquid. These bubbles may be suspended in the liquid or may be trapped in tiny cracks either in liquid's boundary surface or in solid particles suspended in the liquid. The expansion of the minute bubbles may be affected by reducing the ambient pressure by static or dynamic means. The bubbles then become large enough to be visible to the unaided eye. The bubbles may contain gas or vapour or a mixture of both gas and vapour. If the bubbles contain gas, the expansion may be by diffusion of dissolved gases from liquid into the bubble, or by pressure reduction, or by temperature rise. If, however, the bubbles contain mainly vapour, reducing the ambient pressure sufficiently at essentially constant temperature causes an 'explosive' vapourisation into the cavities which is the phenomenon that is called *cavitation*, where as raising the temperature sufficiently causes the mainly vapour bubbles to grow continuously producing the effect known as *boiling*. This means that the explosive vapourisation or boiling do not occur until a threshold is reached.

Hydrodynamic cavitation is produced by pressure variations in a flowing liquid due to the geometry of the system. When the local pressure of a liquid is reduced sufficiently, the dissolved air in the liquid starts to come out of the solution. In this process, air diffuses through cavity walls into the cavity. When pressure in the liquid is further reduced, evaporation pressure of the liquid is achieved. At this point the liquid starts to evaporate and cavities start to fill with vapour. When this kind of a cavity is subjected to a pressure rise cavity growth is stopped and once the pressure

gets higher cavities start to diminish. Cavities disappear due to dissolution of air and condensation of vapour.

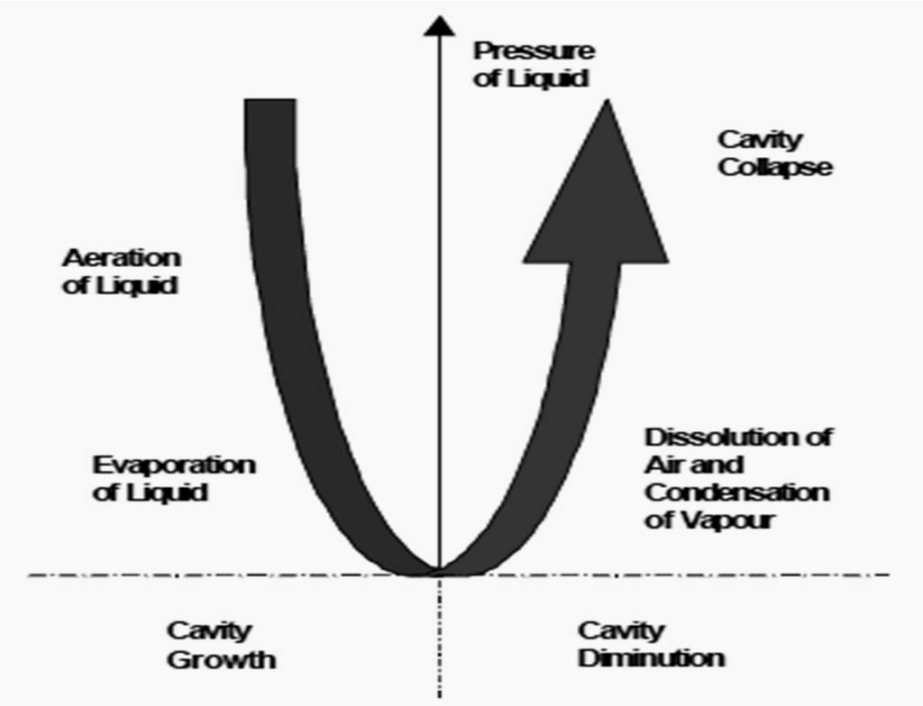

Figure-2.1 *Hydrodynamic cavitation process [21]*

When the cavitation bubbles are carried to higher-pressure regions they collapse. This collapse within the body of the liquid is symmetrical and emits shock waves to the surrounding liquids causing very high pressure pulses. When cavitation collapse occurs near the solid boundaries, the collapse is asymmetrical. This asymmetrical collapse of cavity causes micro-jets of water. If this occurs near mechanical surfaces, it may cause erosion. These violent implosions of cavities produce vibrations that travel through the solid structure.

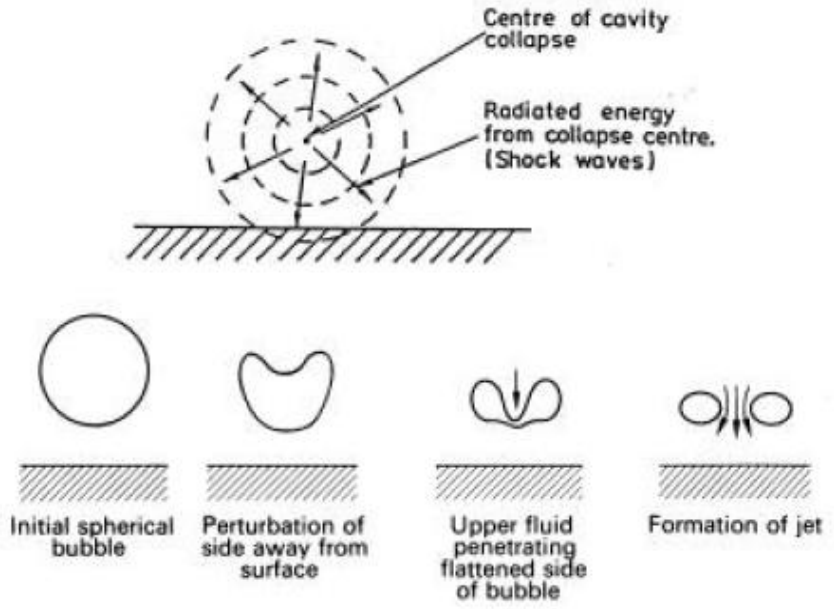

Figure-2.2 *Shock-wave mechanism and micro-jet mechanism of cavitation erosion [21][22]*

In a flowing system, the liquid velocity varies locally and at the points of highest velocity, low pressure and cavities occur. *Cavitation by acceleration* occurs when sufficient acceleration causes the static pressure to drop below the saturation vapour pressure. *Vortex cavitation* occurs in the cores of vortices, which are revolving flows caused by a solid in a liquid. This mechanism takes effect in the liquid itself, whereas the preceding mechanism acts at a liquid/solid interface. Cavitation in this case is due to the drop in pressure caused by centripetal force of the vortex.

Flow cavitation can be further classified as:

Travelling cavitation, which occurs when cavities form in the liquid and travel with the liquid as they expand and subsequently collapse.

Fixed cavitation, which occurs when a cavity or pocket attached to the rigid boundary of an immersed body or a flow passage, forms and remains fixed in position in an unsteady state.

Bubble cavitation, which occurs on solid surfaces with a moderate pressure gradient. Isolated bubbles a formed and then clustered together. Bubbles are carried away by water flow and last only a short time.

Streak cavitation takes place on solid surfaces with high pressure gradient. Streaks increases in size and then break away from the surface, making room for the next streak, and so on.

The degree of cavitation can be estimated with the aid of a non-dimensional parameter typically referred to as cavitation number σ. It is defined as the ratio of static pressure to dynamic pressure that is pertinent to the problem at hand. Cavitation number σ is usually defined as

$$\sigma = \frac{(Ps - Pv)}{\frac{1}{2}\rho V^2}$$

where, Ps is the static pressure at the impeller, Pv is vapour pressure of the fluid, ρ is the fluid density and V is the fluid velocity with respect to the impeller vane. When σ is large, the likelihood of cavitation is small. As σ is reduced, local cavitation occurs near the area of minimum cavitation.

Incipient cavitation is the term used to describe the type and stage of cavitation that is just detectable as the cavitation appears. Cavitation inception number is the value of σ at which cavitation occurs. It is defined as

$$\sigma_i = \frac{(Ps - Pv)}{\frac{1}{2}\rho {V_i}^2}$$

where V_i is the velocity at which cavitation occurs. Depending on the type of cavitation σ_i will vary. When cavitation number is greater than σ_i, cavitation does not occur. When σ drops below σ_i, cavitation begins and increases as σ is lowered.

Although cavitation number σ is widely used in literature it is not generally easy to measure, owing to the difficulty in measuring pressures and local flow velocities near the impeller/stator in a jet unit.

Cavitation occurs frequently in hydraulic machines. It causes vibration, increase of hydrodynamic drag, changes in the flow hydrodynamics, erosion, thermal and light effects (such as luminescence), generation of noise, and acoustic emission.

2.1. Cavitation in water jet propulsion unit

Water jet propulsion systems for watercraft typically have a combustion engine driven pump located within a duct in the hull of the watercraft. An inlet opening for the duct is positioned on the underside of the watercraft. The pump generally consists of a rotating blade row (impeller) followed by a stationary blade row called stator, both located within the duct and followed by a nozzle. A jet of water is pushed

out rearward of the watercraft through the nozzle to propel the watercraft. The rotating impeller absorbs power from the engine, and the stationary blade row and nozzle remove the swirl velocity and accelerate the flow to form the jet.

In fluid power applications the vapour pressure is reached when flow velocity is increased or when there is a significant change in height of a flowing fluid. During periods of high power demand from a water-jet pump, the pressure of the water can decrease to the vapour pressure leading to the formation of vapour bubbles or sheets. When a vessel tries to accelerate from low vessel speed or when high thrust is required at bollard-pull (zero speed) conditions, the high power demand can cause the water pressure in the duct immediately upstream of the impeller to drop significantly, thus contributing to impeller cavitation.

Cavitation is common in water jet units of all size. The formation of the cavitations results in undesirable operation of the jet pump. A part of the mechanical energy is converted into vaporization, sound and vibration and this reduces the overall efficiency of the jet pump. It is when there is large-scale cavitation that there is a problem and when there is significant bubbly cavitation that collapses. Sheet cavitation tends not to upset the efficiency and generally does not cause damage to solid boundaries. In cases where large-scale cavitation occurs, the pump cannot absorb the power from the engine. This causes an increase in engine and impeller rotational speed and tends to increase the extent of cavitation. If the impeller is fully cavitating and the engine is significantly unloaded, the engine power must be limited accordingly to alleviate the cavitation.

3. Cavitation detection: Current methods and techniques

The methods to detect cavitation in real machines are based on the measurement and the analysis of the induced signals. Cavitation detection is made challenging by the noise present in the operating environment due to the internal combustion engine noise, bearing and hull noises, shock and vibration. System variability over time normal wear and marine growth can also affect the ability to detect cavitation. Furthermore, the measured signals can be contaminated by noise coming from other excitation sources of hydrodynamic, mechanical or electromagnetic origin. Therefore, the selection of the most adequate sensor and measuring position on the machine is of relevant importance to improve the detection.

In addition, measurements have to be carried out at different operating conditions to monitor the complete machine operating range. Finally, the measured signals must be recorded with a sufficiently high sampling frequency so that the information in high-frequencies is not lost or aliased.

The most commonly used method for identifying the presence of cavitation in hydraulic machines is based on observations of the drop in efficiency. It must be noted that cavitation starts to develop before the usual “critical” point, the 1% drop in efficiency in turbine model testing. It is generally accepted that the pressure for inception of cavitation is not constant and varies with fluid physical properties and the surface roughness of the hydraulic equipment. Other techniques, such as vibration analysis, hydrophone observations, and application of the high-frequency acoustic emission technique in condition monitoring of rotating machinery have

been growing over recent years. The typical frequencies associated with these techniques range from 3 KHz to 1 MHz.

The interesting trend, where when the cavitation number is decreased, the measured signal first rises, experiences a local maximum, then falls to the local minimum, and rises again [1], is actually well known and was first reported by Pearsall [2] who investigated cavitation noise and vibration in a centrifugal pump. However a thorough explanation of the trend was never given.

The paper by Tomaž Rus et al. [1] explains that a correlation exists between the acoustic emission, vibration, and noise on one side, and topology, type, and extent of cavitation structures on the other side.

Prominent sensing methods used to detect cavitation are described below:

(a) Pressure transducer and Vibration Accelerometer

When cavities are imploded, pressure waves are produced in the surrounding water. These pressure waves can be recorded using high-speed pressure transducers. The propagation of pressure waves continues from fluid to the surrounding component body and measurement of the acceleration of the component surface using accelerometer reveals the presence of cavitation. Often, these vibration signals are contaminated and corrupted by other mechanical impacts or friction, which emits higher frequency noises and occasionally low frequency noises. Referred that the creditable audio bandwidth of the cavitations in turbine is from 3 kHz- ~15 kHz, the

vibration accelerometer sensor is more suitable to monitor the medium/high frequency among the audio bandwidth of cavitations. [1], [4]

(b) Acoustic Emission sensor

The use of acoustic emission sensors serves to extend this analysis to upper frequencies that the accelerometers cannot reach. The information given by the high frequency spectral content sometimes is not conclusive because other excitations such as rubbing can also provoke this symptom [1][4][5][6][10]**.** The amplitude of a given frequency band can be compared for the various operating conditions by computing the auto power spectrum of the time signals. A uniform and sharp increase of this band in comparison with a cavitation-free situation can indicate the presence of cavitation. Moreover ultrasound wavelength is magnitudes smaller, the ultrasound is much more conducive to locating and isolating the source of problems in loud plant environments and not easily contaminated. The advantage of AE technique is the rejection of typical mechanical and process operational background noise (less than 20 kHz).

(c) Hydrophone

Tomaž Rus et al. [1] mention a method of cavitation detection using high-frequency hydrophone submerged in water mounted close to the turbine impeller. It can be used for sound measurements with a frequency ranging from 0.1 Hz to 180 kHz**.** A method of detection of cavitation phenomena in a centrifugal pump using audible sound is explained by M. Cudina [7] using microphones as sensors.

(d) Visualisation

Computer based visualisation is suggested as a possible method of cavitation monitoring is mentioned in [8]**.** This method of the cavitation monitoring was tested on the model Kaplan turbine, where beside the computer-aided visualisation various integral parameters were simultaneously observed. Tomaž Rus [1] also mention cavitation detection by post-processing of images acquired by CCD camera and a stroboscopic light arrangement. A vision-based system for real-time detection of cavitation inception is explained in a paper by Antonio Baldassarre et al.[9]. This method uses a video camera and a PC for real-time detection of cavitation.

Signal processing techniques:

The methods to detect cavitation in real machines are based on the measurement and the analysis of the induced signals. Detection is not an easy task because, depending on the hydraulic machine design and the operating condition, the type of cavitation, its behaviour and its location are different. So, this affects the nature of the excitation and determines the transmission path followed up to the sensor.

Tomaž Rus et al. [1]**,** Abbot, P.A. [11]and Xavier Escaler et al. [5] explain a technique using amplitude demodulation in detecting cavitation in hydro turbine. Amplitude demodulation (envelope analysis) using Hilbert transform is a method of signal analysis, which includes elements of signal treatment in the time and frequency domain. The demodulation procedure has to start with the filtering of the time domain signals in a wide frequency band of about several kHz to remove low frequency content. Then the amplitude envelope of the filtered signal is computed using an algorithm based on the Hilbert transform. Finally, the averaged auto-power

spectrum of several analytic signals is obtained with a high resolution. And the envelope is obtained by forming the analytical signal; that is a complex time signal whose imaginary part is the Hilbert transform of the real part. The analysis of the resulting envelope in the frequency domain permits the identification of frequency values associated with the dynamic behaviour of the cavities.

A method of Full-wave rectification spectral analysis is described by Abbot, P.A. in [4]. In this method, the transfer gain of each turbine installation is determined. This transfer gain is then multiplied with the acceleration signal to obtain acoustic power radiated by the turbine to the vibration at the sensor. The radiated power signal is processed using full-wave rectification spectral analysis. From this analysis, the blade-passage modulation level and index are measured. It is suggested that these quantities are directly related to cavitation unsteadiness.

Cavitation is an unsteady phenomenon that provokes low frequency pressure oscillations and high-frequency pressure pulses. The pressure oscillations are associated with the cavity dynamics and the pressure pulses are produced by the cavity collapses. As a result, vibrations and acoustic noise are generated and propagated through the hydrodynamic and mechanical systems. This low frequency fluctuation can be detected by the use of dynamic-pressure transducers flush-mounted on the draft tube wall. If the intensity of the fluctuation is strong, the detection can also be made from structural vibrations. So, in this case, the procedure only requires the analysis of the frequency content of the pressure and vibration signals within a low frequency range. The above as a possible technique for detecting cavitation in turbine is mentioned briefly by Xavier Escaler et al. [5]

A method to analyse turbine cavitation using wavelet singularity detection is described by WU Yu-lin et al. [18]. Although wavelet analysis is commonly used in image processing, the effectiveness of this method in detecting cavitation in real-world conditions is to be further researched, as there are only a limited number of publications available in this area.

There are also a number of patents in the area of cavitation in marine jet propulsion system. These patents mainly discuss methods to control cavitation. A technique used to prevent the impeller cavitation is suggested by sensing the pressure immediate upstream of the impeller [12]. The jet drive cavitation control system briefly limits engine output power to prevent onset of impeller cavitation when pressure upstream of the impeller indicates the likelihood of imminent impeller cavitation. A threshold cavitation water pressure is pre-selected. When the water pressure drops below this value it sends a signal to the engine controller reducing the engine output to limit the impeller cavitation. Engine power output can be limited by any number of ways, for example, clipping spark plug ignition, retarding spark plug ignition, limiting throttle, limiting amount of air supplied to the engine, limiting amount of fuel supplied to the engine, adding water to the exhaust stream, or modifying the configuration or operation of exhaust port valves (***Figure-3.1***); thus claimed by the patent. The likelihood of impeller cavitation during low-speed acceleration and maneuvering is higher with larger watercrafts, and is also higher when more powerful engines are used.

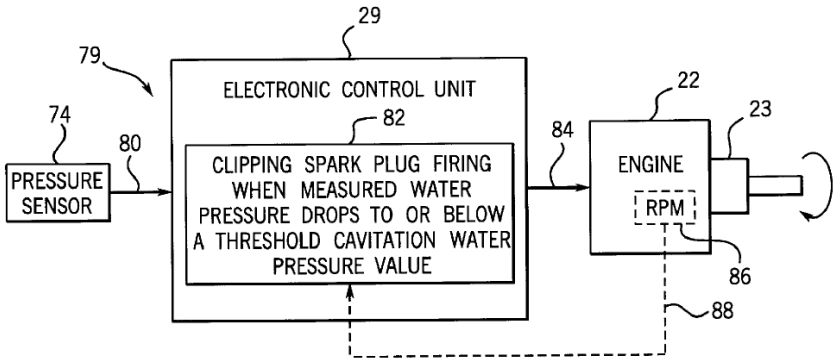

Figure-3.1 *Refer patent [12]*

The patent [13] mentions a control apparatus for controlling the operation of an outboard marine engine. More particularly it relates to such an engine control apparatus which is effective in preventing a reduction in propulsion force due to cavitation (under loaded or idling condition) caused by bubbles produced by a propulsion screw, thereby providing improved acceleration performance. A rotational speed sensor is mounted on the camshaft or crankshaft for sensing the rotation speed. A throttle sensor senses the throttle opening or the degree of opening of throttle valve of the engine corresponding to the quantity of depression of and accelerator pedal of engine by an operator and generates a corresponding throttle signal. A bubble sensor is used to sense the amount of bubbles generated around the propulsion screw and produces a corresponding bubble signal. Based on the output signals of the sensors, a controller generates a drive signal for controlling engine operating parameters in a manner to limit the number of revolutions per minute of the engine when the speed limiter determines that the amount of bubbles is equal to or greater than a predetermined value **(*Figure-3.2*)**.

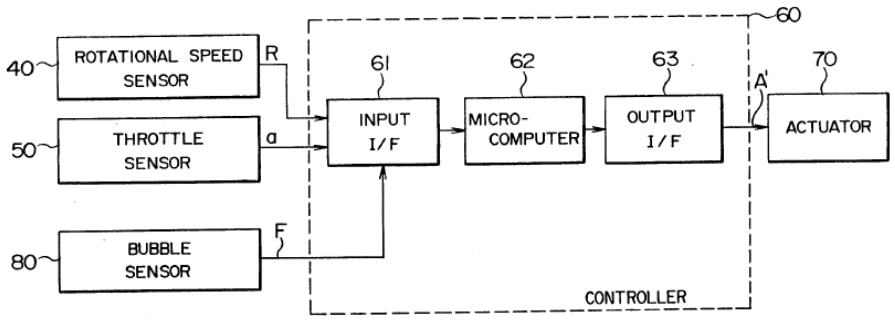

Figure-3.2 *Refer patent [13]*

The patent [14] describes a technique to control cavitation by sensing the rate of rise of engine speed. If the throttle is fully opened and rate of rise of engine speed is a predetermined value or more, a delay control is applied to the rise.

Another patent [15] describes a method of implementing anti-cavitation by sensing the propeller slip. The inventor claims that the relationship between the ideal slip and boat speed could be determined empirically and can be used by the boat manufacturer as a guide for improved performance. The determination of slip can be done by measuring the propeller rpm and the boat speed. This slip information can be used to control the motor power to within an acceptable slip range.

U.S. Patent [16] mentions a similar method of cavitation detection by sensing the dynamic pressure within the pump. The dynamic pressures are measured and compared with the known cavitation alarm pressure. The cavitation alarm dynamic pressure is a known percentage of non-cavitation dynamic pressure. When the measured dynamic pressure is determined to be less than the cavitation alarm pressure, an indicator is made available.

U.S. Patent [17] describes placement of one or more pressure sensors (which comprises a tube for generating venturi vacuum signal) that create a mechanical signal that is conducted through a vacuum line (similar to a venturi tube) and then converted into an electric signal to indicate pressure. This water pressure signal provides appropriate feedback signal for the interruption of a spark to the engine.

4. Experimental set-up

Although the cavitation detection has received a great deal of attention, it is still very difficult to detect and predict the cavitation intensity accurately. Moreover the presence of hull noise, conducted noise from the second jet unit and other noises ambient noises make the detection problem in jet boat very challenging. Hence it was decided to first conduct tests on a controlled and less noisy environment such as the in-house test-rig facility to obtain cavitation related signal characteristics in a jet unit.

The experiments to acquire cavitation related signals were conducted in two different test sites. Firstly, data was recorded from the experimental test rig facility at Hamilton Jet and secondly the test was conducted on a jet boat in real-world conditions. Since the aim of this project was to develop a low cost sensing technique that could be used for production in future, sensors and data acquisition systems with very high price were avoided. This made the vibration and pressure measurements as viable sensing methods to detect cavitation. Moreover, the location of the occurrence of cavitation in a water jet made it impractical to use such methods as visualisation and use of hydrophone.

The following sensors were used to record signals during the experiments.

4.1. Sensors used in tests

4.1.1. Knock sensor

A Bosch KS-R automotive knock sensor was used for detection of high-frequency vibration noise. The Bosch knock sensor was selected for the experiment since it was of low cost, available off the shelf and had a similar characteristic of an accelerometer. This sensor has a moving mass which exerts compressive forces on an annular piezo-ceramic element in time with the oscillation producing the excitation. These forces cause a voltage to be generated between the top and bottom of the ceramic element. This voltage is measured using a very high impedance voltage amplifier. The Bosch knock sensor has a bandwidth of 1 kHz – 20 kHz with a sensitivity of 26 ± 8 mV/g which can measure vibrations in the range of 0.1…400 g.

4.1.2. Pressure sensor

A Kistler 4075A10 pressure sensor was used to measure the static as well as the dynamic absolute pressure in the test rig. It can be used for pressure measurement from 0...10 bar absolute and has a natural frequency of more than 45 kHz. It has a sensitivity of 50mV/bar. Pressure acts on a thin steel diaphragm with a silicon measuring element. The latter contains diffused piezo-resistive material connected in the form of a Wheatstone measuring bridge. The effects of pressure unbalance the bridge and produce an output signal of 0 ...500mV full-scale. The measuring bridge in the sensor is fed with constant calibration current of 2...5 mA. The measuring amplifier supplies the calibration current generating a full range signal of 0...500 mV. The pressure sensor is screwed directly onto the test-rig with diaphragm of the

sensor in contact with the water.

4.1.3. Accelerometer

The accelerometer used for the cavitation tests was B&K Type 4333. The transducing element consists of two piezoelectric discs on which is resting a heavy mass. When the accelerometer is subjected to vibration the mass exerts a variable force on the piezoelectric discs. Due to piezoelectric effect a variable potential is developed across the discs, which is proportional to the acceleration of the mass. The accelerometer has an undamped natural frequency of 60 kHz and is calibrated to have a frequency bandwidth of 20 kHz. It has a voltage sensitivity of 17.8 mV/g, charge sensitivity of 19.3 pC/g and maximum shock acceleration of 10,000 g typical.

4.2. Data acquisition system

Since the test facility included the test-rig at the company and jet-boat in real-world condition, it was important that the data acquisition system used was portable. The tests included acquiring data simultaneously from multiple type sensors installed at different locations on the test facility. A high-accuracy NI-9233 C-series analog module from National Instruments was used during the test. The module has 4 channels and can sample input voltages from all channels simultaneously at 50 k Samples/seconds. The input side of each channel has a Sigma-Delta type ADC with a resolution of 24 bits with an idle channel noise of 95 dBFS at 50 kS/s. Input signal range to each channel is ± 5V with the typical excitation current of 2.2 mA. The input signal connectors of the module are standard BNC type. The sampled data output from the module was stored in the portable computer via a USB cable. The LabVIEW SignalExpress interactive software from National Instruments was used to

configure and store data on to the computer from the data acquisition module.

4.3. Test procedures and set-up

The following discussion provides a description the sensor installation, instrumentation and procedures used for the cavitation detection tests conducted on the test-rig facility at the company site and on the test boat.

4.3.1. Sensor location

Three different sensors were used on the test facility at Hamilton Jet - an accelerometer, a knock sensor and a pressure sensor. All the sensors were installed at positions close to and around the impeller such that they can measure the pulses produced in the water flow due to cavitation, with a high degree of response.

For the tests conducted on the test boat, two knock sensors were used at two different sensor positions since we were not sure which location would provide a clear cavitation signal. The use of pressure sensor and the accelerometer in boat tests were avoided due to the installation difficulties on the boat. Moreover, it was found from the test-rig test that both the accelerometer and the knock sensor produced very similar responses to cavitation. For the tests on boat, the first knock sensor was fixed on to the transom flange and the second one on the inspection cover on the jet unit. **Figure- 4.1** shows the sensor installation positions on the boat.

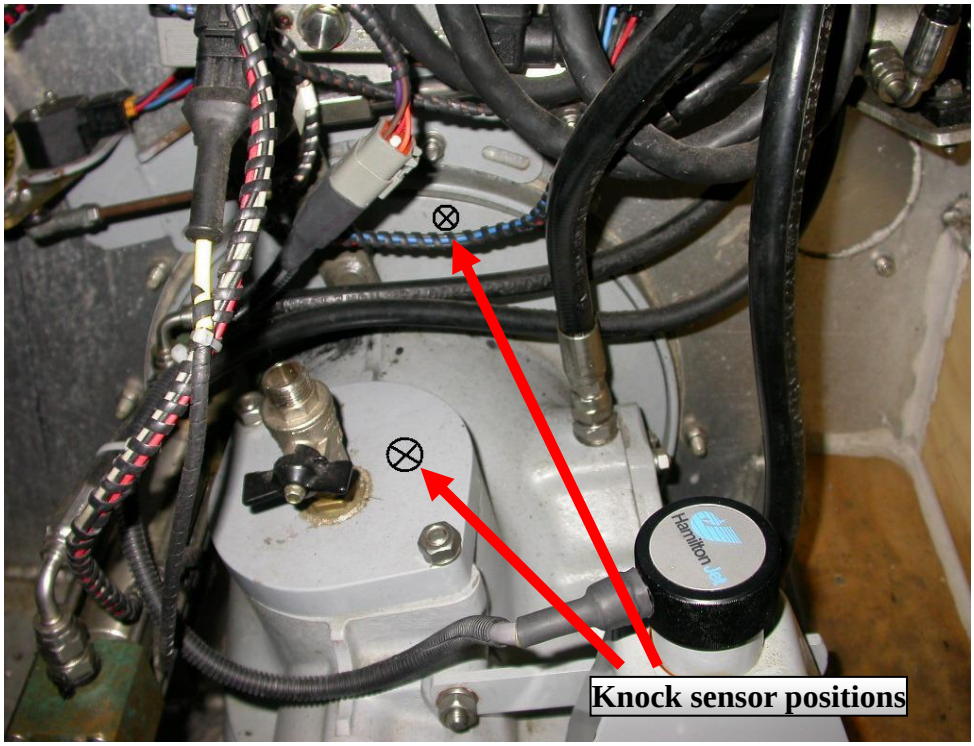

Figure-4.1 *Knock sensor mounting positions on the boat*

4.3.2. Instrumentation

The instrumentation used to measure the cavitation related signals during the operation of the test-rig at Hamilton Jet is shown in **Figure- 4.2**. The output from the sensors were amplified separately to a suitable signal level using a charge or voltage amplifier and fed directly to the data acquisition system. The accelerometer is connected to the B&K Type 2624 low-noise charge amplifier using a miniature coax cable. The output signal of the amplified to ±5V is connected to one channel of NI-9233 data acquisition (DAQ) module. The Bosch knock sensor is connected to a custom-made charge-amplifier through a twisted-pair cable and the charge-amplifier output is fed to another channel of DAQ module. Similarly the signals from the Kistler pressure sensor is amplified and given to one channel of the DAQ module.

The signals from the aforementioned sensors are sampled simultaneously at a rate of 50 kS/s. The DAQ module is connected to the laptop via a USB cable and data is recorded using LabVIEW SignalExpress software. The sensors, the signal conditioning amplifiers and the DAQ module were kept very close to each other to reduce unnecessary cable length and the induced ambient noise.

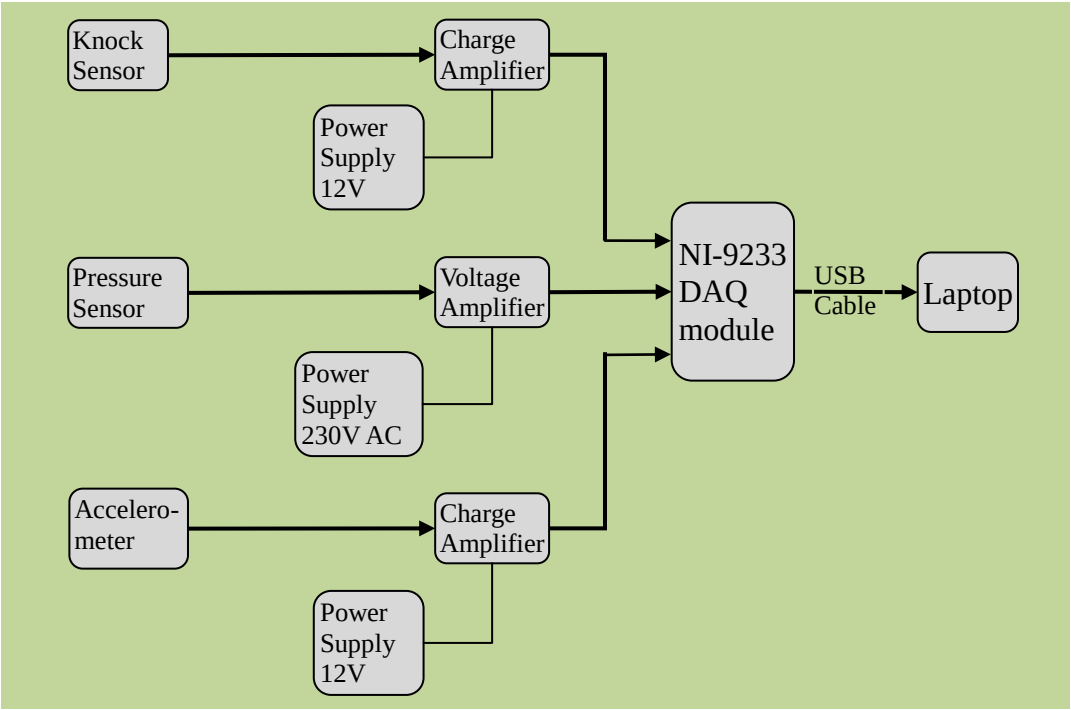

Figure-4.2 *Block diagram of instrumentation for test-rig test*

The block diagram of the instrumentation set-up for tests conducted on the jet boat is shown in **Figure- 4.3**. Only two knock-sensors installed at two different positions of the jet-unit were used during the boat-tests to log cavitation related vibration signals. The knock sensor and the instrumentation used during the test were same as the one used for tests conducted on the in-house test facility at Hamilton Jet. In addition to that, the engine RPM is also recorded for additional data analysis. The pulse signal from the RPM sensor is level-shifted using a resistor voltage divider and fed to one

channel of the NI-9233 DAQ module. The onboard 12V DC voltage source is used to supply power to the charge amplifier, which is designed to accept voltage in the range of 10-20V. The knock sensor signal conditioner is kept near to the mounted knock sensors. The DAQ module was fixed firmly on to the boat frame such that the cable length to the sensor signal conditioner was kept low. A 5-meter USB active extension cable was used between the DAQ and the laptop. Similar to the test on the in-house testing facility, LabVIEW SignalExpress was used to record data on the computer.

The amplifier and signal conditioners used to process the signals from the sensors were calibrated and verified for frequency response and usable bandwidth to make sure they comply with the sensors used in the experiments.

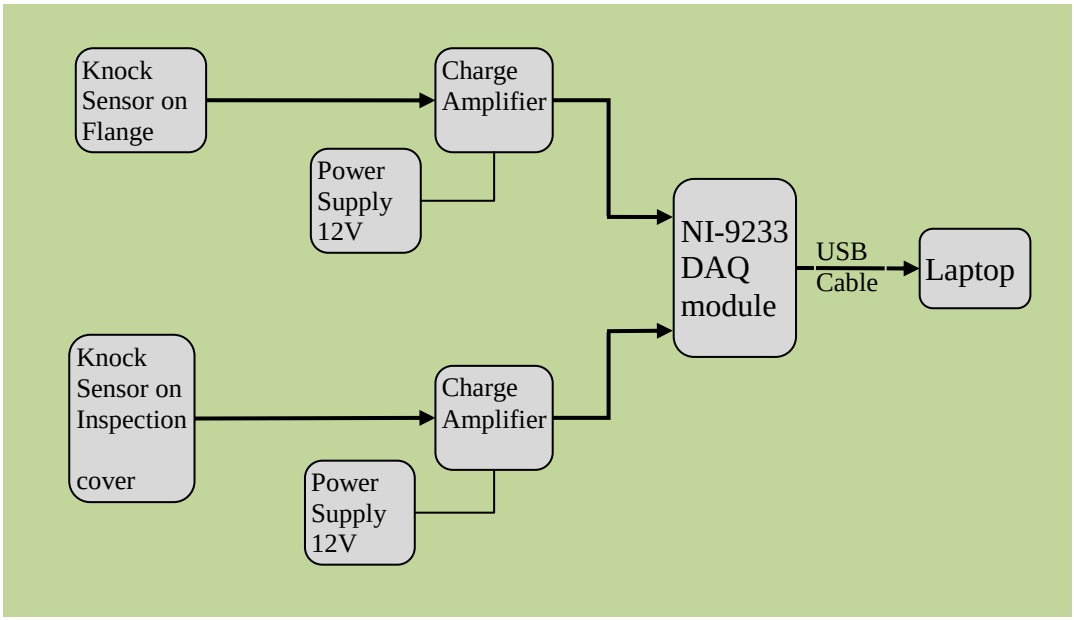

Figure-4.3 *Block diagram of instrumentation for Boat tests*

4.3.3. Test procedure

A series of tests were conducted to record cavitation related signals on the in-house test-rig facility and on the test boat, under various operating conditions. No

frequency modifiers or filters were used while recording the sensor signals so that possible loss of information during signal conditioning was minimized.

The test rig experiments were conducted with RPM and the static water-pressure inside the test-rig as variable parameters while sensor signals were recorded. The control-computer at the test-rig facility is used to vary the RPM of the impeller. The water-pressure is monitored using the pressure gauge, which shows the static pressure inside the rig in Inches of Mercury (inHg). Data were collected for different static pressures in the rig while keeping RPM constant. The experiments were repeated for various values of RPM. Sensor signals for transient pressures were also recorded while reducing the test-rig pressure by draining the water out of rig using a control valve. For transient tests, the time required for the rig static pressure to change from a ‘no-cavitation pressure’ of 14 psi to a ‘full-cavitation pressure’ of 12 inHg absolute vacuum pressure was around 30 seconds. Constant-pressure tests were also conducted by varying the RPM with the control computer. Transient-RPM data was also recorded keeping test-rig pressure as parameter. Refer to Appendix-I for the complete test plan for the test-rig experiments. The test-rig was fitted with a Perspex window so that cavitation could be visually observed during the tests.

For the boat-test, the engine RPM and boat speed were the only readily available parameters that can be controlled to create cavitation condition. Therefore the tests were designed to record cavitation data under various combinations of the RPM and boat-speed, recording data for both static and transient conditions of the aforementioned parameters. The tests were repeated to record data from both the knock-sensors installed on the transom flange and the inspection cover of jet unit.

The engine RPM and boat-speed were measured from the instrument panel display and the onboard computer in the boat respectively.

Although the boat has two jet units, only one jet unit was used in the experiment in order to avoid the effects of possible noise that may be induced to the measurement due to the operation of a second jet engine. The reverse-bucket was engaged in different degrees to control boat speed. The idle engine-speed (idle-rpm) was 750 rpm which was the minimum RPM at which we could operate it. At around 1500 rpm the engine turbo-charger cuts-in that may further induce engine vibration noise components to the sensor signal. Refer to Appendix-II for a detailed test-plan of boat-experiments. Note that no method of verifying the occurrence of cavitation on the boat is available, other than the visual observation of the phenomenon. Hence cavitation was inferred from the boat and engine operating conditions such as high audible noise and vibration.

5. Results and discussions

This section presents the data analysis and the detection algorithm developed from the tests conducted on the in-house test-rig facility and the test boat. The result from the test-rig data analysis is presented first, followed by the test boat analysis results.

5.1. Data analysis methods

The first objective of the data analysis was to determine a suitable frequency range in which the cavitation signatures can be identified. To achieve this, the data was bandpass filtered at different bandwidths and power spectral estimation was performed on each resulting signal. Spectral estimation was performed using the nonparametric periodogram method. The signal energy in each frequency band was calculated and plotted against varying RPM as well as static pressures. The energy in the signal is calculated as

$$\boldsymbol{E = \int_{f1}^{f2} PSD(f)\, df}$$

where $\boldsymbol{PSD}$ is the power spectral density of the filtered signal and $\boldsymbol{f_1}$ and $\boldsymbol{f_2}$ are the lower and upper limit of the bandpass filter. The intensity of cavitation is considered to be directly proportional to the energy $\boldsymbol{E}$ of the signal in the frequency band of interest.

The sensor signals were band-pass filtered to four different frequency bandwidths, viz. 0 - 5 kHz, 5 - 10 kHz, 10 – 15 kHz and 15 – 20 kHz for the purpose of spectrum analysis to obtain cavitation signatures. The above frequency bands were selected for the easiness of performing analysis.

Figure-5.1a and **Figure-5.1b** below show the time-domain signals from the knock sensor mounted on the test-rig at different levels of cavitation. Figure-5.1a is when the test-rig is non-cavitating and Figure-5.1b is when it is heavily cavitating. Signals shown below are recorded at different times but under similar operating conditions. In the time-domain, the signals look very similar except that the amplitude of signal peaks in Figure-5.1b is almost 10 times that of Figure-5.1a. The severity of cavitation was observed through the perspex window fitted on the test-rig.

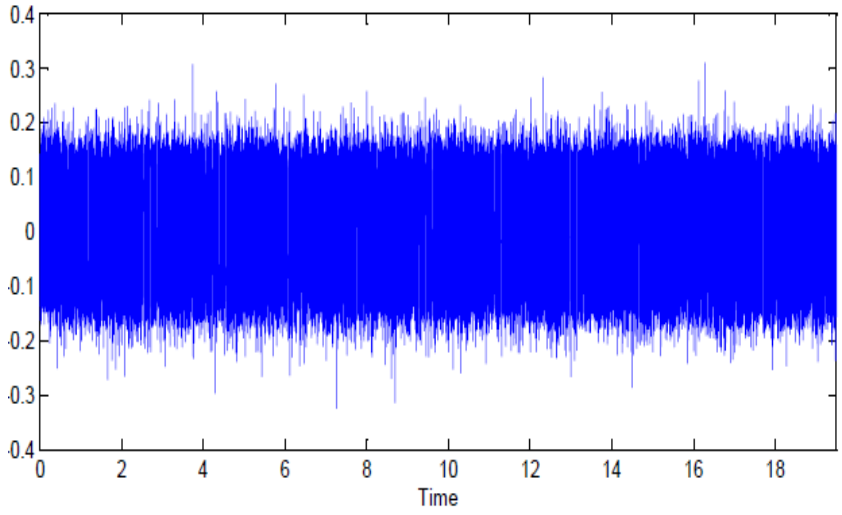

Figure-5.1a *Knock sensor signal - non-cavitating*

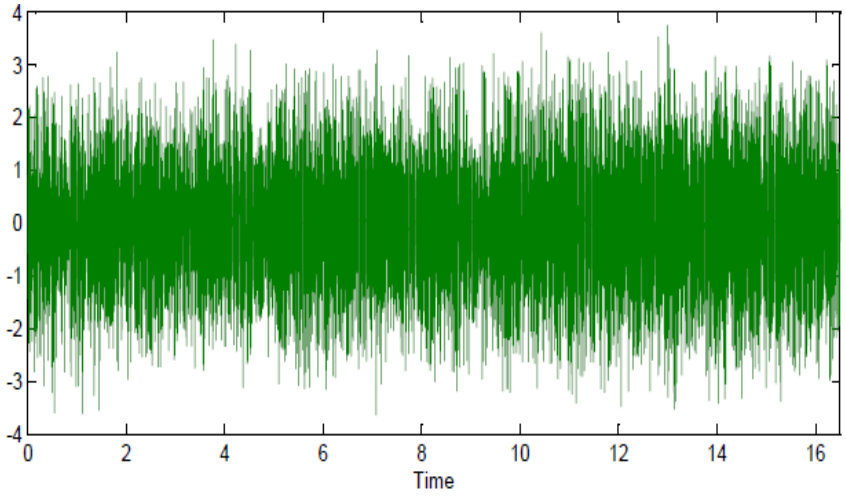

Figure-5.1b *Knock sensor signal - heavily cavitating*

5.2. Test-rig data analysis

To obtain cavitation signatures, the power spectrum of the test-rig data at different levels of cavitation were analysed in the frequency domain. The data were collected from the test-rig running at constant low speed of 1350 rpm and the highest speed of 1760 rpm. The jet unit model used to collect data was HJ-292. The static pressure in the test-rig was reduced from around 14 psi (no cavitation) to 18 inHg of gauge vacuum (heavy cavitation). Note that 18 inHg gauge vacuum is equivalent to absolute pressure of [30 inHg (typical atmospheric pressure) – 18 inHg] = 12 inHg pressure absolute (i.e. the larger the static pressure in *inHg gauge vacuum*, the smaller the actual *absolute pressure* in the test-rig.)

At 1350 rpm, no significant cavitation was observed until the pressure was reduced to the minimum value. The amplitude of the sensor signals was also very low. At

1760 rpm, the severity of cavitation appeared to be increasing with reducing pressure. At 1760 rpm when test rig pressure was reduced more than 10 inHg gauge vacuum, we could visually observe cavitation bubbles through the perspex window. Cavitation also produced more and more noise in the audible range while reducing pressure. With pressure reduced to around 15 inHg below atmospheric pressure at 1760 rpm, an audible noise was produced, sounding much like gravel being sucked into the jet unit.

The spectral analysis of sensor signals indicates that the high frequency cavitation noise in the signal kept increasing while reducing the pressure, especially in the range 10 - 20 kHz. At very low pressures of test-rig (severe cavitation), the high frequency noise spread into a larger frequency band of 5 - 25 kHz.

Figure-5.2 shows spectral density of Knock sensor signal at three different pressures. In Figure-5.2, the spectrum of the signals is plotted for the same linear scale so that the frequency effect of cavitation is clearly visible.

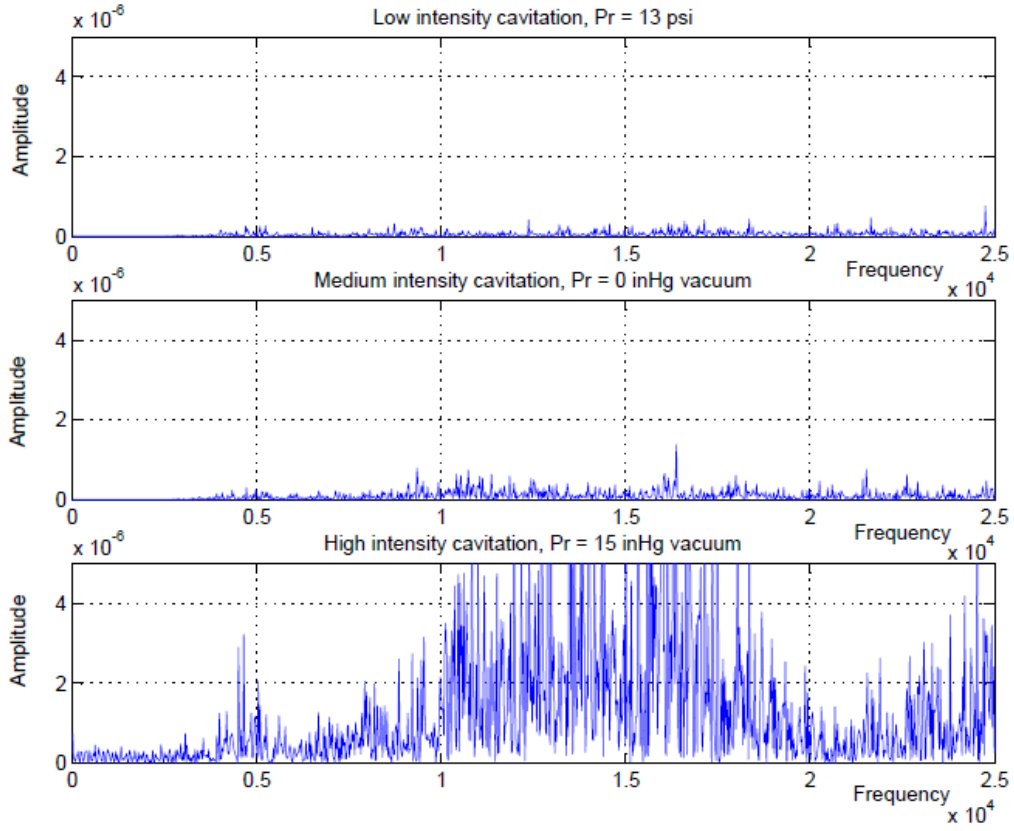

Figure-5.2 *Spectrum of Knock sensor signal at three different static test rig pressures of 13 psi, 0 inHg gauge vacuum and 15 inHg gauge vacuum*

In the low frequency range of 0-5 kHz, blade passage frequency (BPF) components and related harmonics were substantial and the frequency effects of cavitation were not clearly visible. Note that BPF frequency varies with each jet unit and is a function of impeller blade and stator vane numbers.

The data from the sensors were also analyzed for the energy contents in different frequency band to learn the effects of pressure on the cavitation intensity. Note that in *Energy vs. Pressure* plots, the negative values of pressure on the horizontal axis represent the gauge vacuum pressure in inHg.

Figure-5.3 below shows the *Energy vs. Pressure* plot for knock sensor signal for three different frequency bands. As obvious from the figure, vibration sharply increases when pressure goes more than 10 inHg gauge vacuum (i.e. pressure goes below 20 inHg Absolute). Cavitation increases monotonically until it reaches a local maximum, then it gets reduced in intensity until it reaches a local minimum and again increases as pressure is further reduced. This trend is clearly visible in frequency bands of 10-15 kHz and 15-20 kHz. The above trend in energy variation is well documented in literature [1] [2] and is a known characteristic of cavitation. A hypothesis for the phenomenon is that the cavitation grows to a point where it "chokes" itself- the pressure waves emitted by bubble collapse is attenuated in a highly compressible bubbly flow region.

Figure-5.4 shows the variation of pressure sensor output to the static pressure in the test-rig. As with the knock sensor, pressure sensor output also increases in amplitude when static pressure is decreased. Note that for the pressure sensor the lower frequency band of 5 – 10 kHz seems to contain high intensity energy components of cavitation. This is due to the fact that the pressure sensor could measure cavitation pressure pulses directly from water where as knock sensor response output was affected by the properties of the solid medium through which vibration was transmitted. As mentioned above, a similar pattern of reaching a local maximum and local minimum of cavitation is observed in 10-15 kHz and 15-20 kHz regions, although it is not that prominently visible in the latter frequency band for the pressure sensor.

The cavitation intensity in terms of signal energy is also plotted against impeller

rpm**. Figure-5.5** and **5.6** show variation of energy with respect to the inverse-rpm of the test-rig. As the impeller rpm is increased (1/rpm decreases), the sensor signal energy also increases. The pattern of reaching a local maximum can be seen from the plots; the rate of increment of energy with respect to (1/rpm) slows down around 1600 rpm and steadily increases again. The energy is calculated for 10-15 kHz bandwidth for three different static pressures of in the test-rig. Both the knock sensor and the pressure sensor signals are plotted.

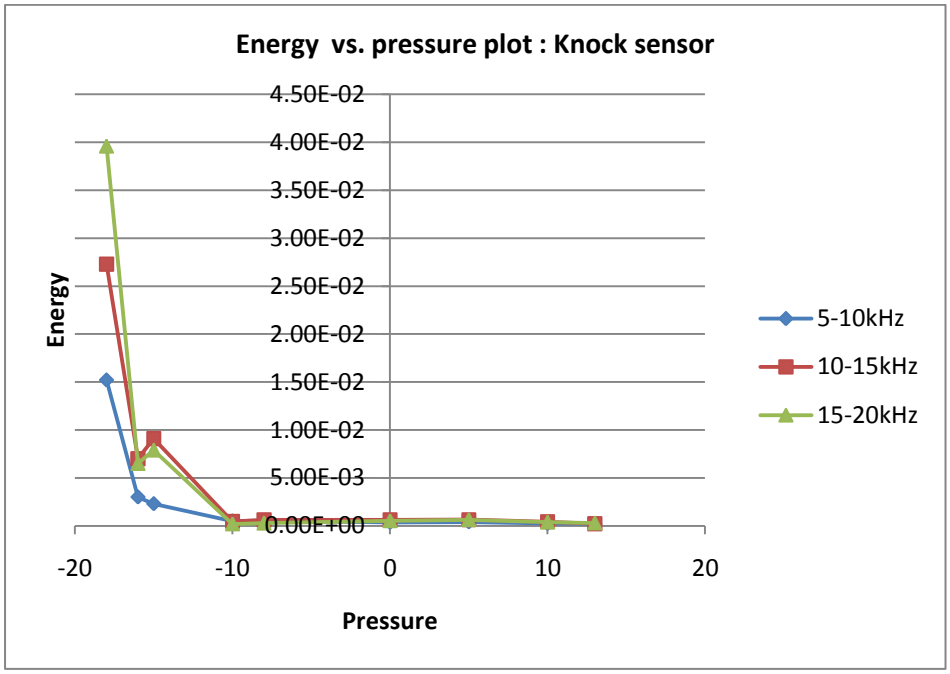

Figure-5.3 *Energy vs. Pressure plot for Knock sensor*

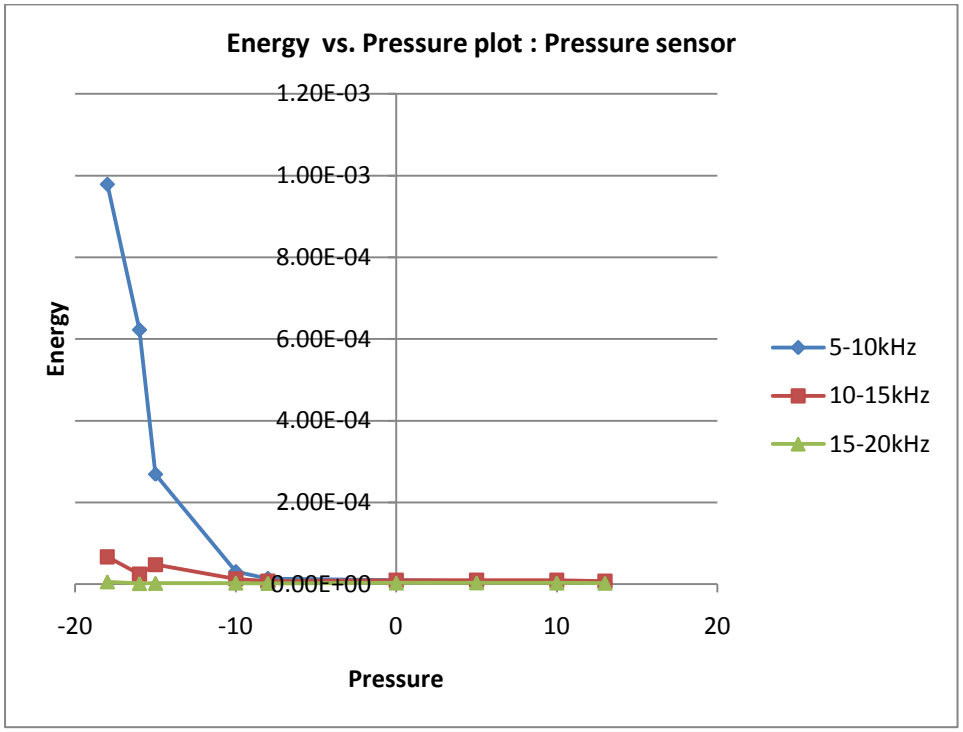

Figure-5.4 *Energy vs. Pressure plot for Pressure sensor*

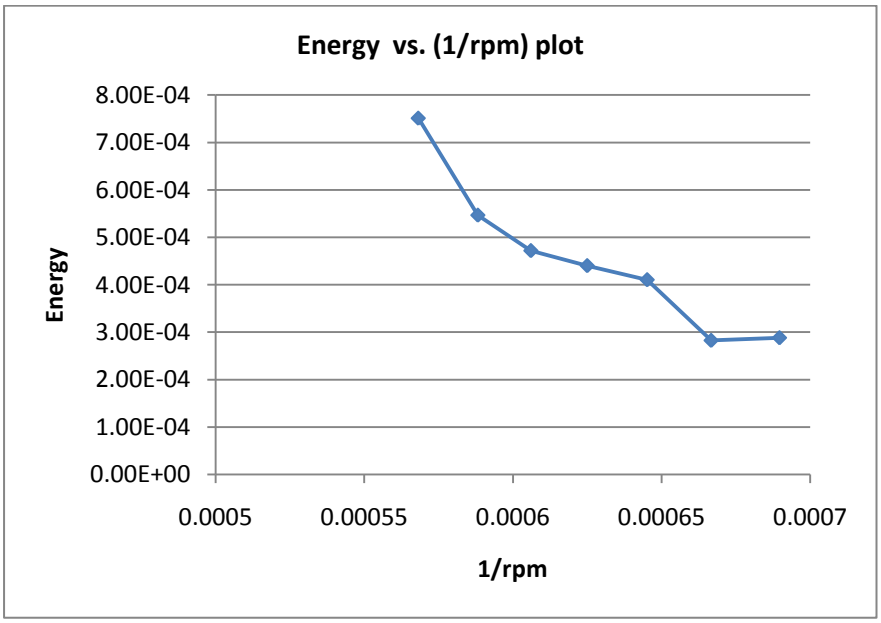

Figure-5.5a *Energy vs.(1/rpm) plot for Knock sensor, at test-rig static pressure of 0 psi gauge vacuum*

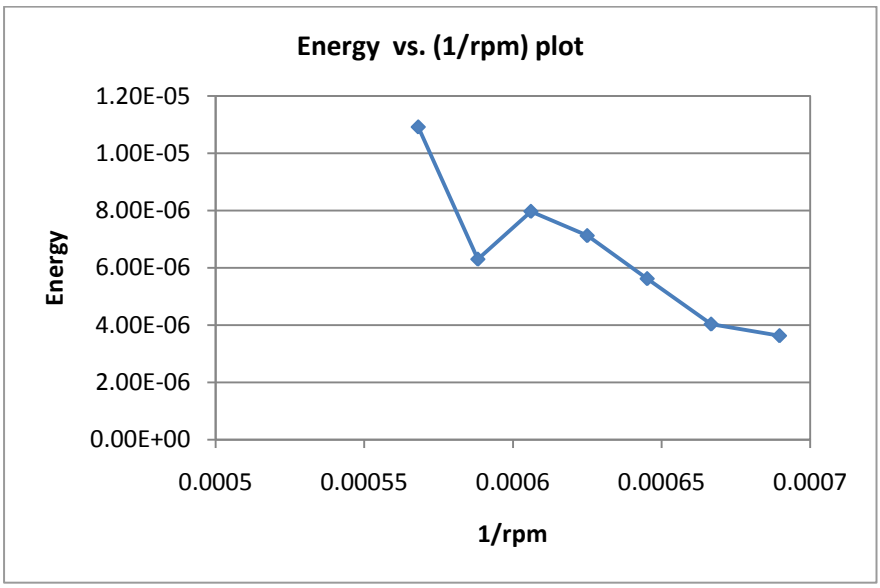

Figure-5.5b *Energy vs. (1/rpm) plot for plot for Pressure sensor, at test-rig static pressure of 0 psi gauge vacuum*

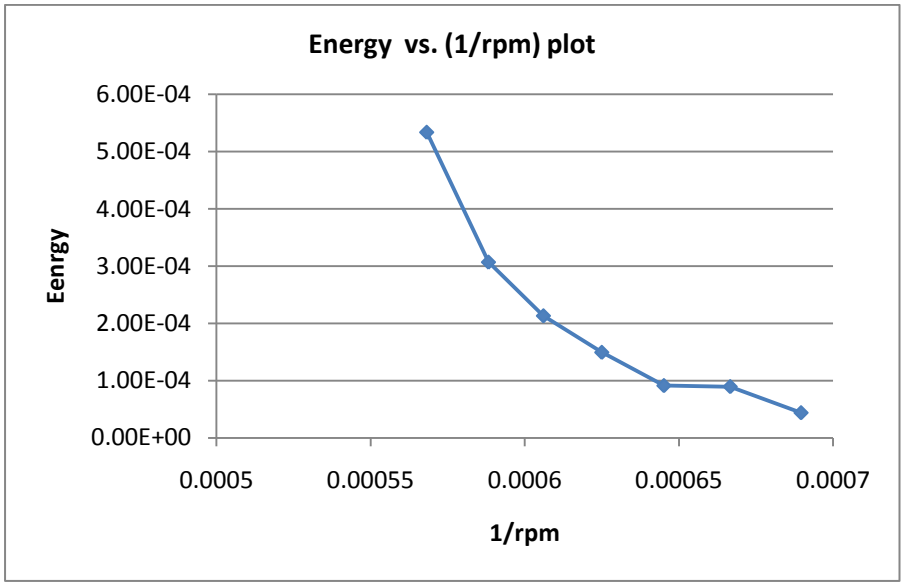

Figure-5.6a *Energy vs. (1/rpm) plot for Knock sensor, at test-rig pressure of 10 inHg gauge vacuum*

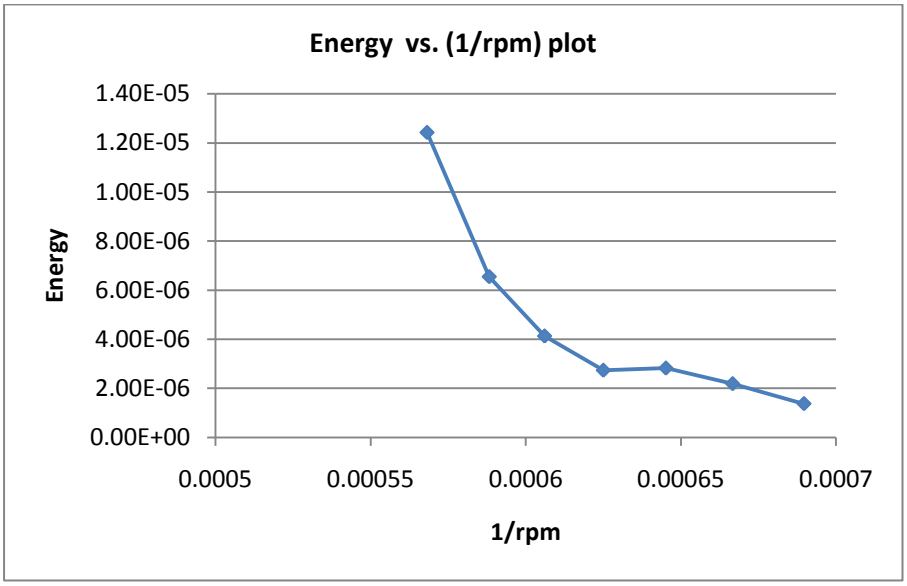

Figure-5.6b *Energy vs. (1/rpm) plot for Pressure sensor, at test-rig static pressure of 10 inHg gauge vacuum*

5.3. Boat data analysis

Since the best location to record cavitation related signals was not known a priori, it was decided to use two knock sensors at two different locations. One sensor was fixed to the transom flange and the second one on the inspection cover. Data was recorded running the boat at different engine rpm as well as at different vessel speeds as it was impossible to vary the pressure independently as on the test rig.

Signals from both sensors were analysed for spectral content using a 2048-point FFT algorithm in Matlab. **Figure-5.7** and **Figure-5.8** show spectral density of signals mounted on the inspection cover and transom flange respectively, for three different engine speeds. The Knock sensor on the transom flange (Fig-5.8) seemed to pick up vibration other than cavitation related ones. As a result, signal from the sensor on the

flange had more noise than the sensor on the inspection cover. This is also evident from Figure-5.7 and Figure-5.8 that are plotted at two different amplitude scales. This made the inspection cover of jet unit to be a better position than the transom flange to observe cavitation signals.

As in the case of the test-rig, the energy variation in signal at three different frequency bands was also analysed. **Figure-5.9** and **Figure-5.11** show *Energy vs. (1/rpm)* when the boat is held stationary by engaging the reverse bucket. **Figure-5.10** and **Figure-5.12** show variation of signal energy with respect to (1/rpm) when the boat is moving at a speed of 5 knots.

The figures show that the energy in the signal rises abruptly when the engine rpm is more than 2250 rpm, indicating onset of cavitation above this point. It can be seen from the figures that the energy rises very fast as engine rpm is increased beyond 2250 rpm, then rate of energy rise slows down reaching a local maximum and again increases sharply when rpm is increased further. Such a similar trend in energy-variation is observed in the test-rig data analysis too, as shown in Figure-5.5 and Figure-5.6. The abovementioned trend in cavitation is found to be more prominent in frequency bands of 10-15 kHz and 15-20 kHz.

Note that when boat is stationary (Fig-5.9 and Fig-5.11), there are more random variations in the energy trend than when boat is moving (Fig-5.10 and Fig-5.12). The spectral analysis also showed that the sensor signals when the boat is stationary tend to have more noise than when the boat is moving. This extra signal noise could be due to the fact that engagement of the reverse bucket reflected the water pushed out

from the jet unit back into the jet intake, which additionally induced more aeration and flow noise.

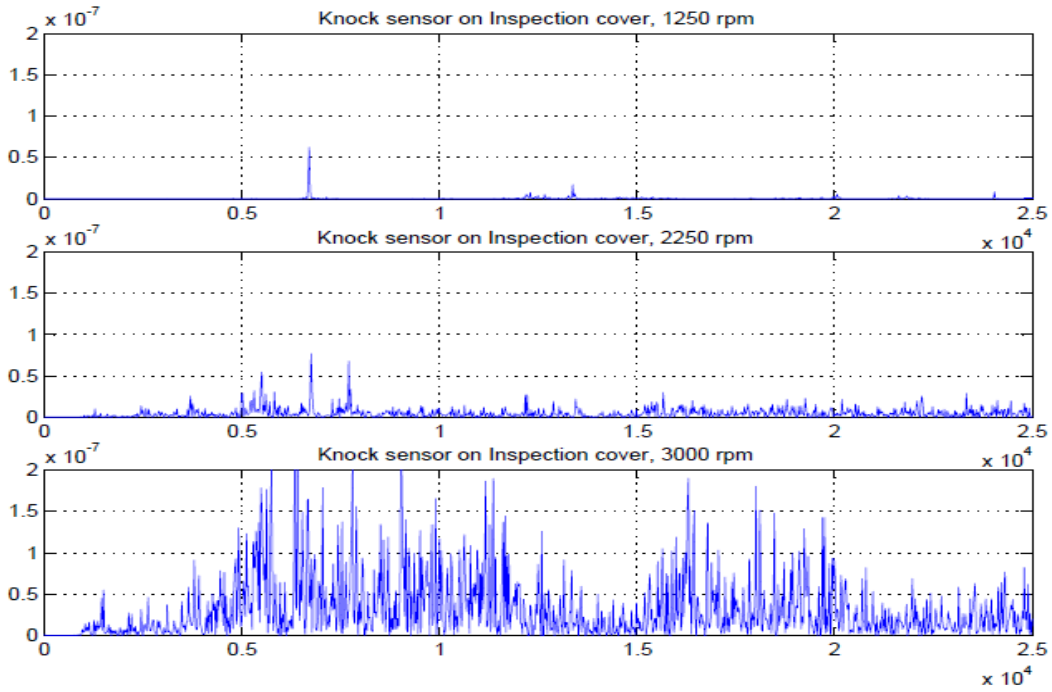

Figure-5.7 *PSD of sensor signal on inspection cover on boat*

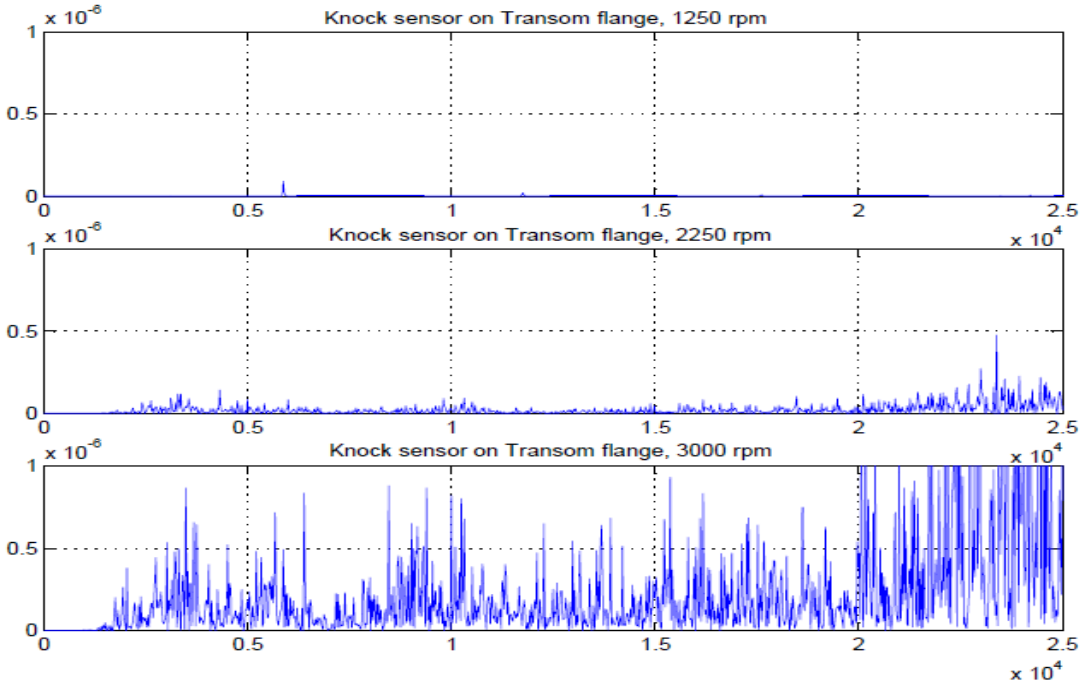

Figure-5-8 *PSD of sensor signal on transom flange on boat*

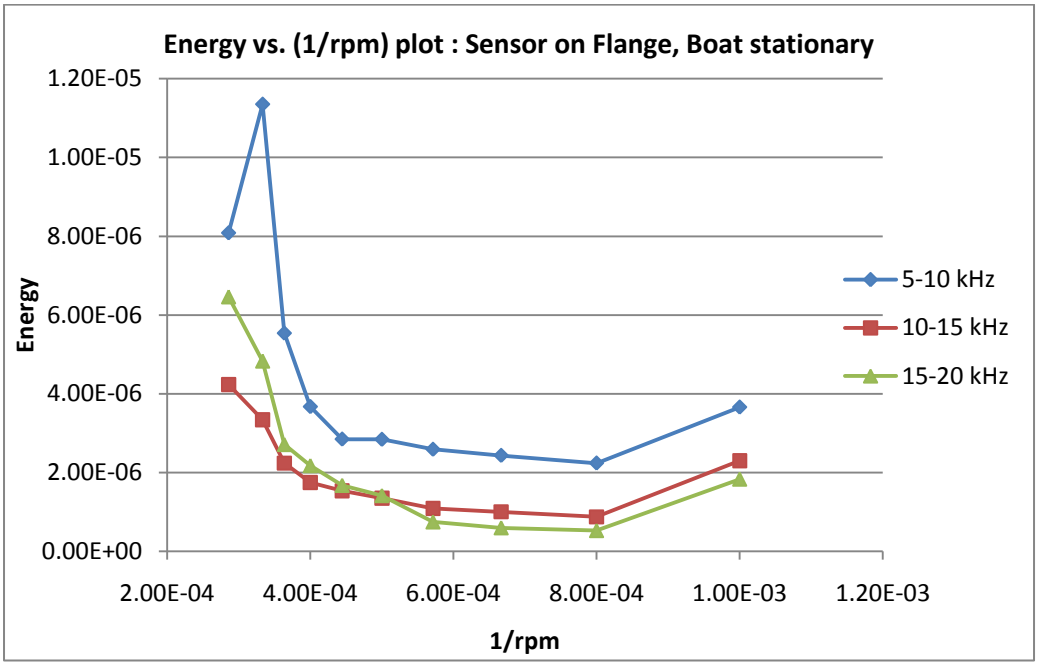

Figure-5.9 *Energy-(1/rpm) plot, sensor on flange, with boat stationary*

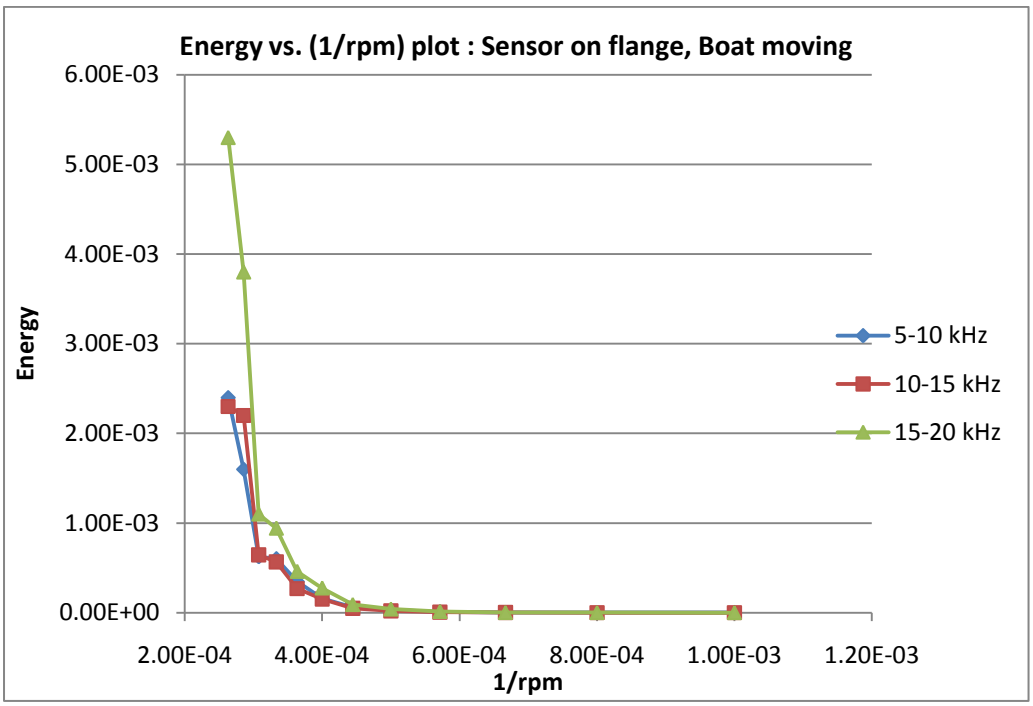

Figure-5.10 *Energy-(1/rpm) plot, sensor on flange, with boat moving*

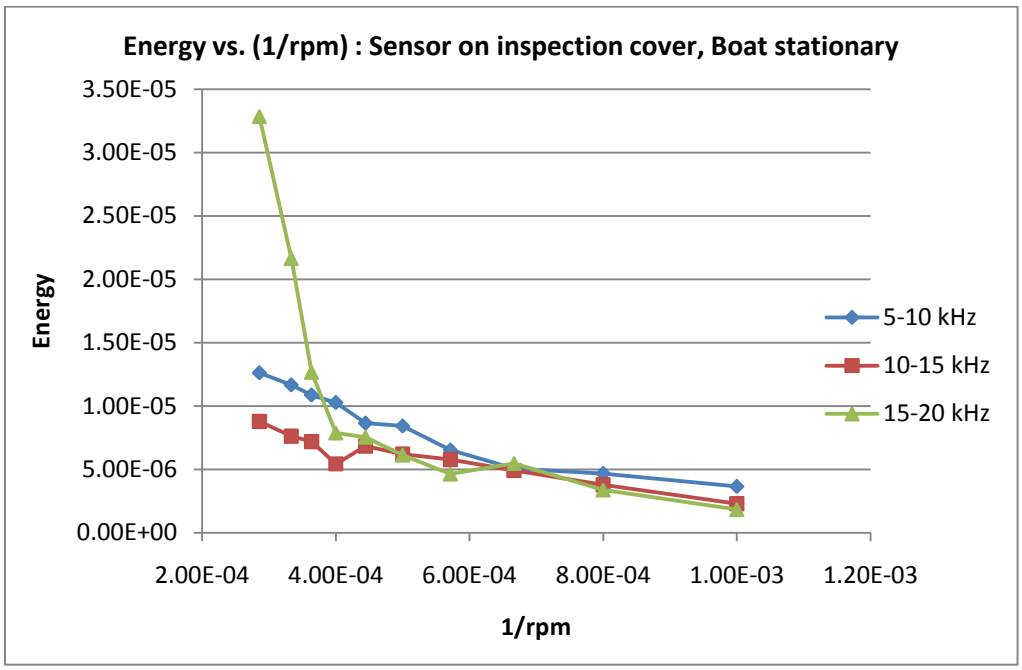

Figure-5.11 *Energy-(1/rpm) plot, sensor on inspection cover, with boat stationary*

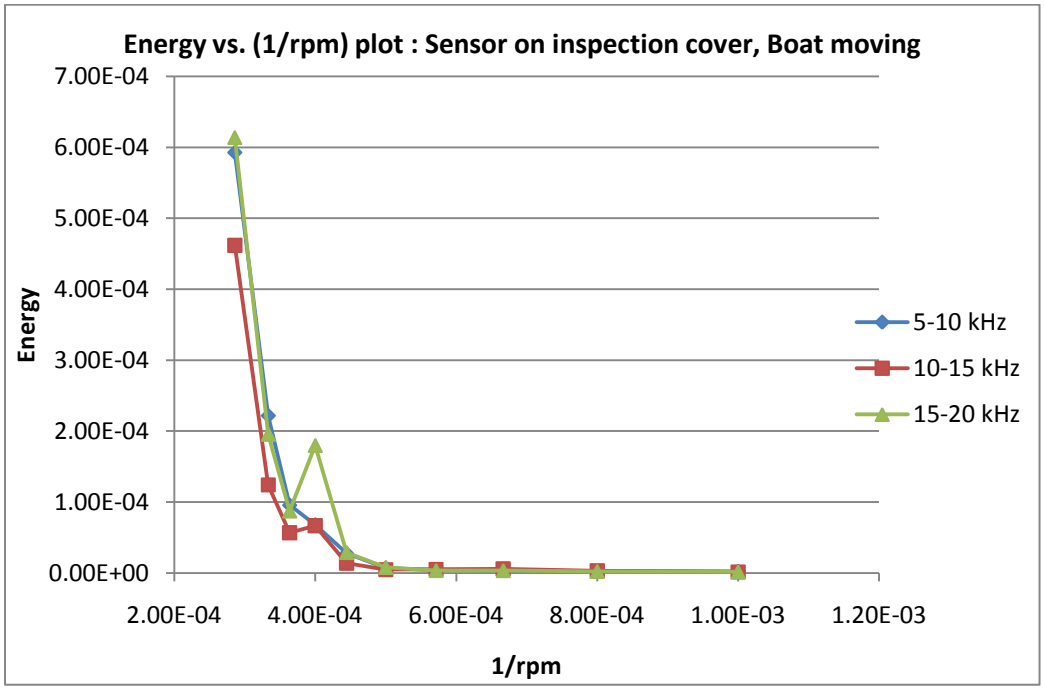

Figure-5.12 *Energy-(1/rpm) plot, sensor on inspection cover, with boat moving*

Summarizing the key findings of the data analysis, the signals recorded from the sensors on the test-rig and boat were analysed in the frequency domain for possible signatures of cavitation. In the case of the test-rig, the energy in the signal increases sharply when the static pressure is reduced below 10 inHg gauge vacuum (which is equivalent to 20 inHg pressure absolute). Figure-5.5a and Figure-5.5b indicate that for the rig pressure of 0psi gauge vacuum, cavitation is beginning to occur around 1500 rpm. Figure-5.6a and Figure-5.6b suggest that when the rig pressure was further reduced to 10 inHg gauge vacuum, cavitation occurred even before the speed reached 1500 rpm. For the boat, the signal-energy increased suddenly when the engine rpm was increased above 2250 rpm. This sudden increase in signal energy proves that there is maximum possibility that the cavitation occurred above 2250 rpm. Apart from that, the huge presence of bubbles in the water-jet pushed out from the jet unit and the high audible noise and vibrations produced above this rpm also underscored the above conclusion. The variation in signal energy with respect to the pressure and engine rpm showed a trend of reaching local maximum and minimum, a phenomenon known to relate to cavitation origin and observed by early researchers in this field. This observation in energy variation further underlines the assumption that the energy contained in the signal can be considered a good estimate of cavitation intensity. This trend is found to be more visible in high-frequency bands of 10-15 kHz in case of test-rig and both 10-15 kHz and 15-20 kHz in case of boat. This variation in frequency band could be due to the difference in size and mechanical properties of the jet units used for test at in-house facility and the boat.

6. Cavitation detection algorithm and simulation results

This section describes the algorithm to detect cavitation, the Simulink model and the results of the simulation.

6.1. Cavitation detection algorithm

Since the development of cavitation in a jet boat is a non-stationary and nonlinear phenomenon, developing models of cavitation accurately would require Computational fluid dynamic (CFD) methods and nonlinear estimation techniques. Given that the aim of this project is to develop an efficient and cost effective solution to detect cavitation, such a method would not be appropriate.

Based on the findings from the literature study, a few time-domain algorithms were developed and tested with the data collected from the test-rig, viz. Hilbert transform based envelop detection and windowed-moving-average method. Although it seemed promising in controlled environments such as test-rig, it failed to produce intended results in boat test. Another method of cavitation detection based on wavelet transform was also analysed but later abandoned due to the complexity of implementation and lack of similar work done in related field.

On the basis of spectrum analysis results described in the previous section, the energy in the sensor signal is taken as an estimate of the amount of cavitation occurring in the jet unit. Based on this, an algorithm is developed and a Simulink model has been created and tested using the recorded data from the test-rig and boat.

Figure-6.1 shows the system diagram of the cavitation detection algorithm. The sampled data from the sensor is first filtered to the frequency of interest using a digital bandpass (BP) filter. In practice it is filtered to a frequency range between 10 kHz and 20 kHz. After the BP filter, the energy in the signal is calculated by computing the power spectral density of the signal. The energy in the signal is then calculated using the formula

$$\mathbf{E} = \int_{\mathbf{f1}}^{\mathbf{f2}} \mathbf{PSD(f)\ df}$$

The energy signal is smoothed using a lowpass filter before passing though a derivative block to avoid instantaneous amplitude variations at the output of derivative block. The calculated energy signal is then compared with the threshold values $\mathbf{E_{th}}$ and $\mathbf{E'_{th}}$ to produce error signals. The signals after the threshold comparison are normalised to provide two error signals $\mathbf{Y_n}$ and $\mathbf{Y'_n}$ whose magnitude varies between 0...1. The type of normalization used is scalar multiplication, which is linear. Hence the algorithm gives two signals; one that is proportional to the cavitation and the other is the rate of change of cavitation. Thus the algorithm implements a proportional and derivative behaviour. These two signals can be combined with appropriate weighting to produce a single signal or given separately as the inputs to the subsequent control logic of the jet unit to control cavitation.

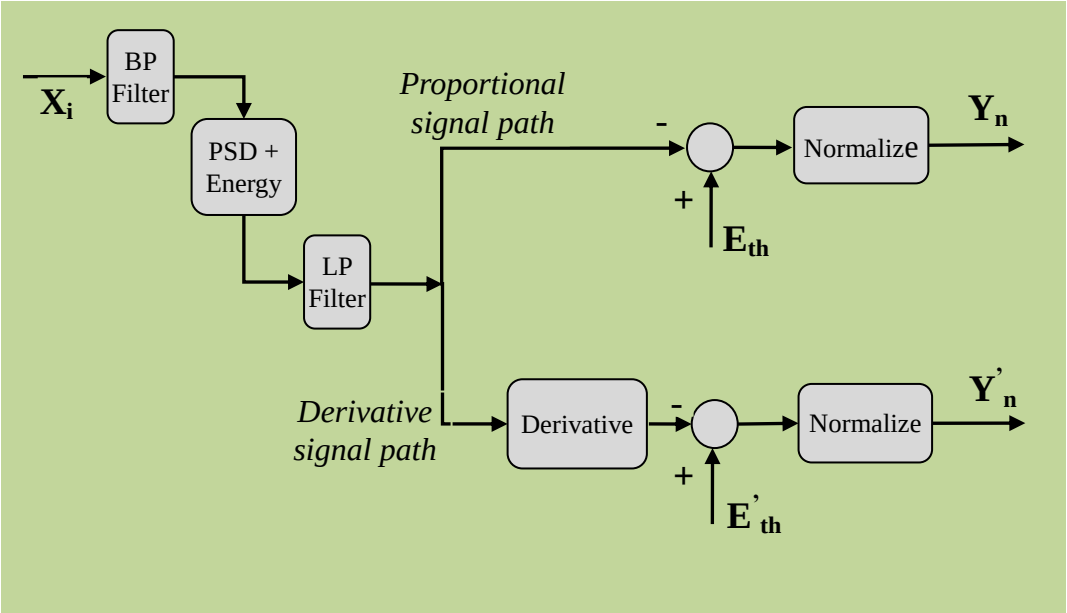

Figure-6.1 *System diagram of the cavitation detection algorithm*

The threshold values E_{th}, E'_{th} and the specifics of the normalisation blocks vary and are dependent of the type and size of jet units used. This can be obtained by calculating energy in the sensor signal when the jet unit is beginning to cavitate, visually observing cavitation during the tests. The signals are normalized by dividing the signals by the maximum energy value in the energy-signal or the derivative of the energy signal, which are already smoothened by the lowpass filter. Since the jet unit at the in-house facility and on the jet boat were of different size, corresponding threshold values were different in the Simulink simulations used for test-rig and boat test data. The threshold and normalisation values of a particular jet unit can be found out at the time of testing a new jet unit model.

6.2. Algorithm simulation and results

The Simulink implementation of the algorithm discussed in the previous section is

shown in **Figure-6.2**. The sensor signal is imported from the workspace of Matlab with S*ample time* set to 0.00002 (which is DAQ sampling period, 1/Fs) and *Samples per frame* of 2048. So the output is frame based with a frame size of 2048 and frame period of 0.04096 seconds. The input data is filtered using a bandpass FIR filter with passband frequency 10-15 kHz. In the next block, the energy contained in this frequency band is calculated using periodogram method, 2048-point FFT. The output energy signal from this block is smoothed using a lowpass (LP) FIR filter. This LP filter has pass-band cut-off frequency of 1 kHz and transition band of 4 kHz with pass-band ripple of 1dB and stop-band attenuation of 100dB. The lowpass filter is designed in such a way that it gives optimum response with minimal signal distortion and delay.

Figure-6.3 shows the signals generated at different points in the Simulink model. The input is the signal from the Knock sensor, when the boat engine rpm is changed abruptly from the idle-rpm of 750 rpm to maximum of 3800 rpm and again back to idle-rpm, keeping the boat stationary.

The top plot in **Figure-6.3a** shows the signal just before and after the lowpass filter in Simulink model. The green-coloured curve is the calculated signal-energy input to the LP filter and red-coloured curve is the output of LP filter. Bottom plot in Figure-6.3a signals before and after threshold comparison for the proportional signal-path. It generates output $\mathbf{Y_n}$ (blue-coloured signal) that is proportional to the intensity of cavitation. Note that $\mathbf{Y_n}$ turns more negative as cavitation grows.

Figure-6.3b shows the normalised signals before and after threshold comparison for the derivative signal-path, for the same input signal. It generates output $\mathbf{Y'_n}$ (blue-coloured signal) that is the rate-of-change of intensity of cavitation.

Output signals $\mathbf{Y_n}$ and $\mathbf{Y'_n}$ are given to the subsequent boat control scheme to control cavitation.

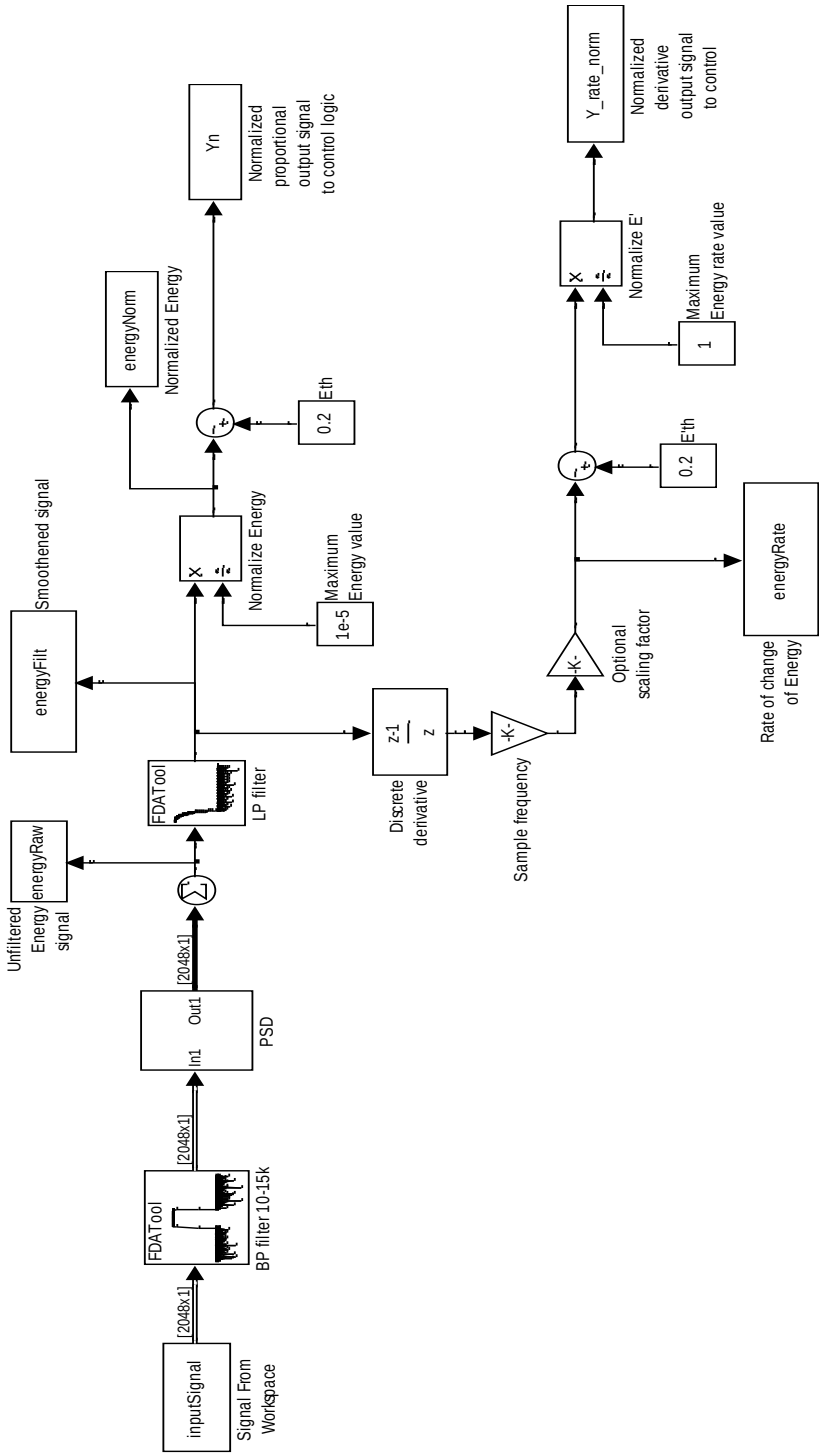

Figure-6.2 *Simulink implementation of the algorithm*

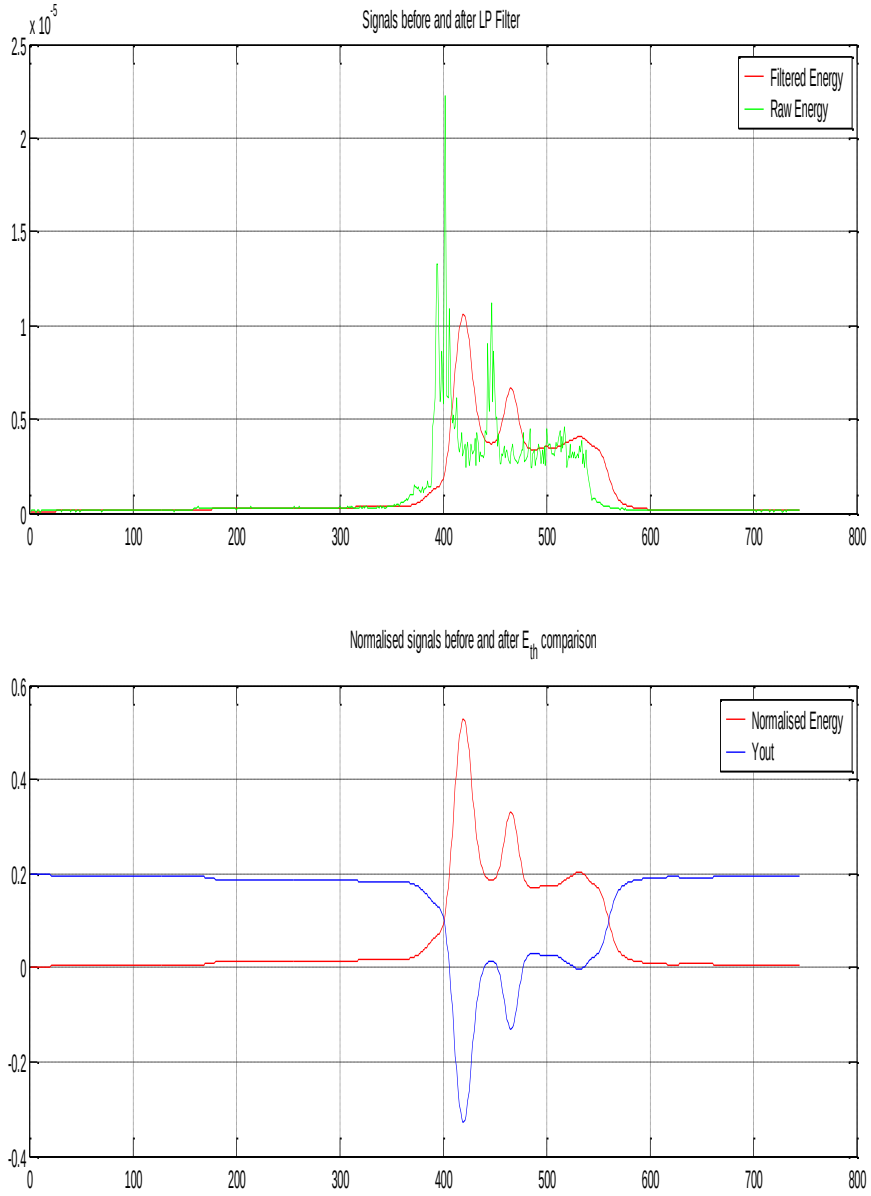

Figure-6.3a *(Amplitude-time plot) Top-plot shows input (green) and output (red) signals of the lowpass filter block. Bottom-plot shows signals before (red) and after (blue) threshold comparison for proportional signal-path Simulink model, with* $\boldsymbol{E_{th}}$ *= 0.2. Input is Knock sensor signal from boat test.*

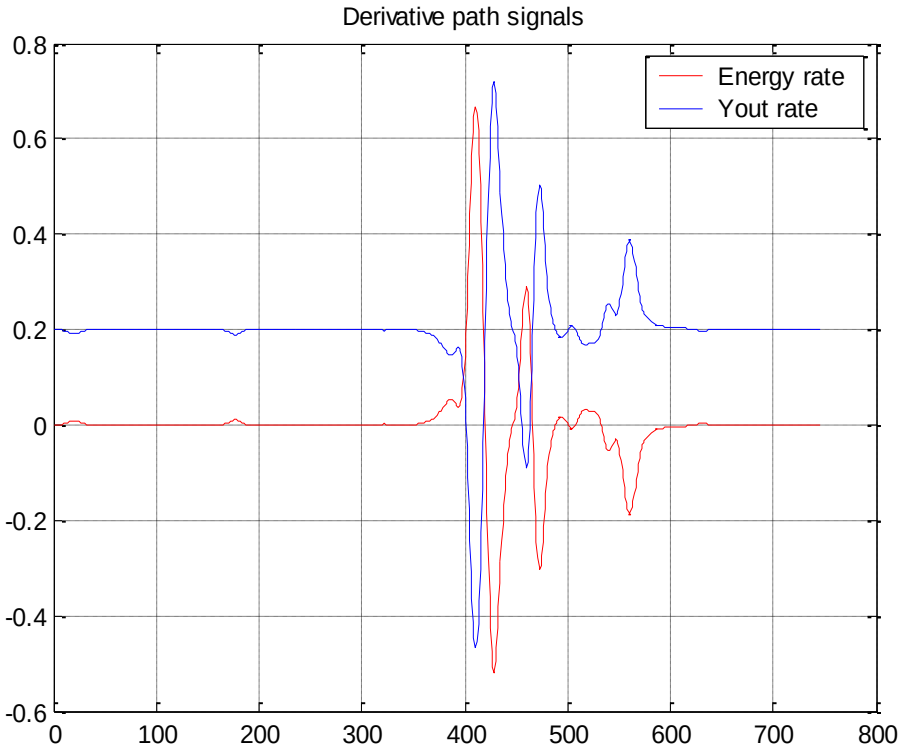

Figure-6.3b *(Amplitude-time plot) Blue-coloured signal is the derivative-output of the algorithm with* $E'_{th} = 0.2$.
Input is Knock sensor signal from boat test.

Similar to the Figure-6.3, **Figure-6.4a** and **Figure-6.4b** show signals generated by the cavitation detection algorithm with input being signal from Knock sensor on the test rig. In the test-rig, the static pressure is decreased from 14 psi (no cavitation) to 14 inHg gauge vacuum (heavy cavitation). As rig pressure goes low, cavitation also increases progressively.

Figure-6.5a and **Figure-6.5b** show similar signals generated by the Simulink model with a Pressure sensor signal given as input to the algorithm, for the same test as in Figure-6.4.

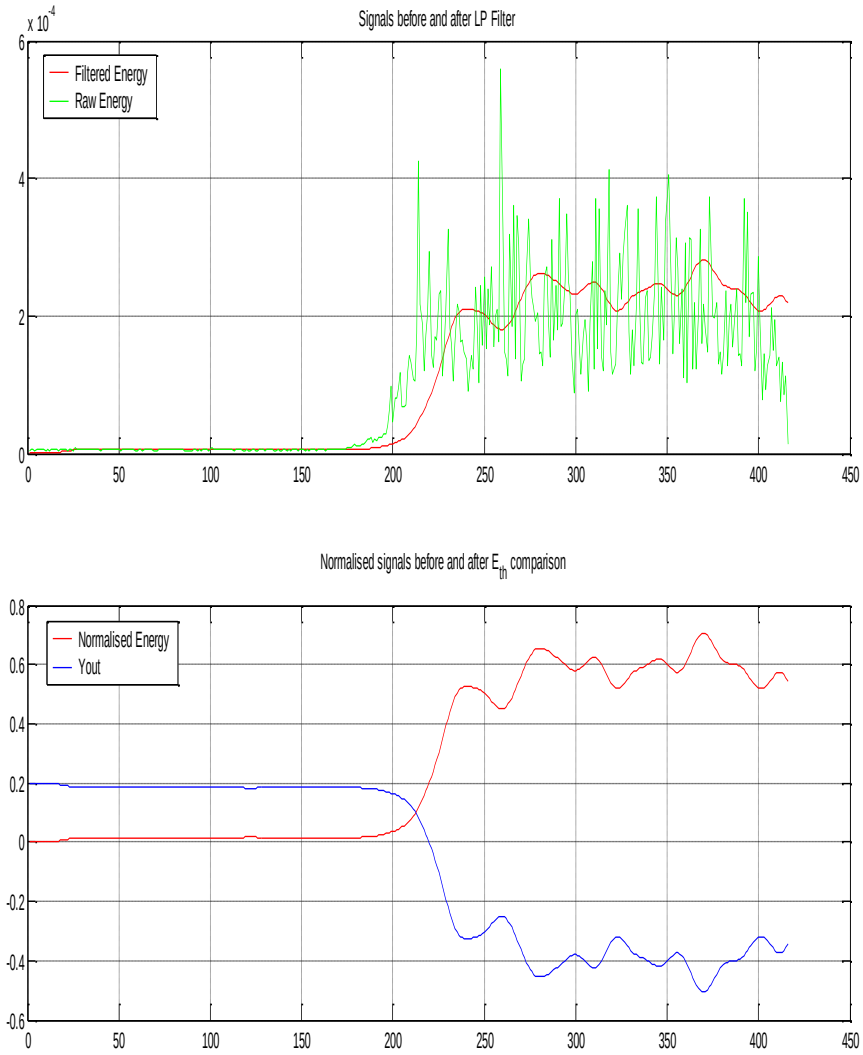

Figure-6.4a *(Amplitude-time plot) Top-plot shows input (green) and output (red) signals of the lowpass filter block. Bottom-plot shows signals before (red) and after (blue) threshold comparison for proportional signal-path Simulink model, with* E_{th} *= 0.2. Input is Knock sensor signal from test rig.*

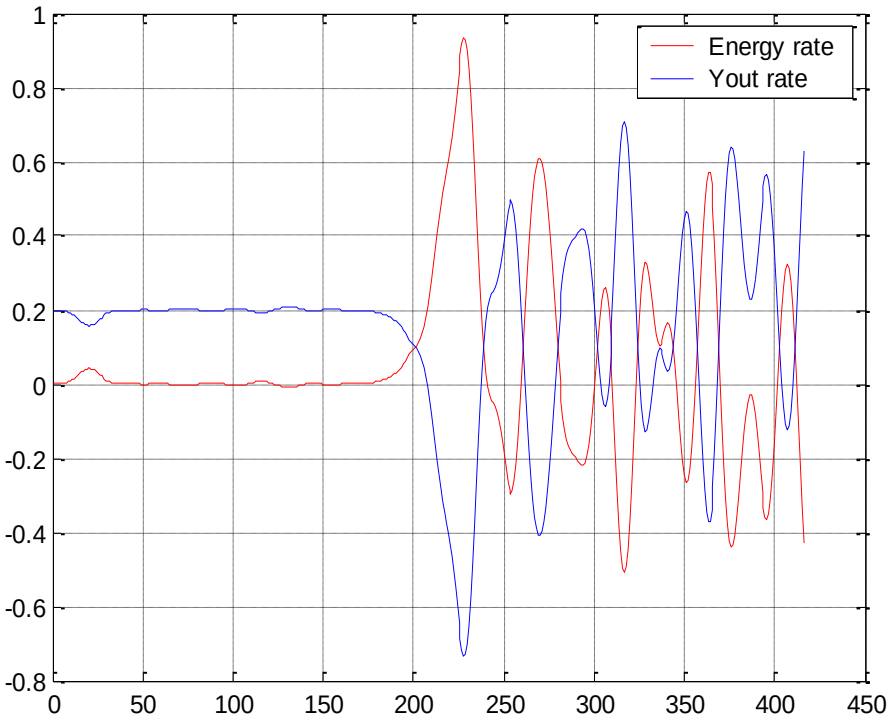

Figure-6.4b *(Amplitude-time plot) Signals before (red) and after (blue) threshold comparison in the derivative signal-path in Simulink model, with* $E'_{th} = 0.2$*. Input is Knock sensor signal from test rig.*

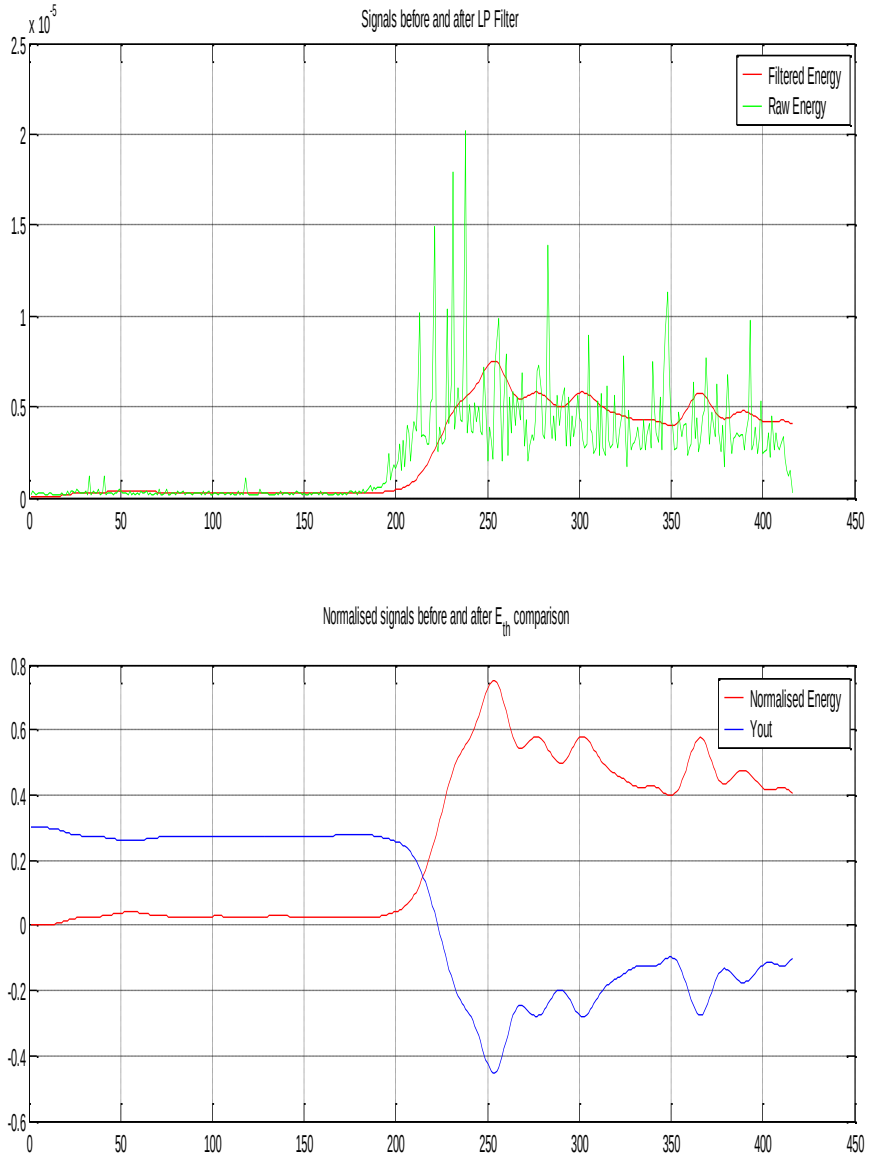

Figure-6.5a *(Amplitude-time plot) Top-plot shows input (green) and output (red) signals of the lowpass filter block. Bottom-plot shows signals before (red) and after (blue) threshold comparison for proportional signal-path Simulink model, with* $\boldsymbol{E_{th}}$ *= 0.3. Input is Pressure sensor signal from test rig.*

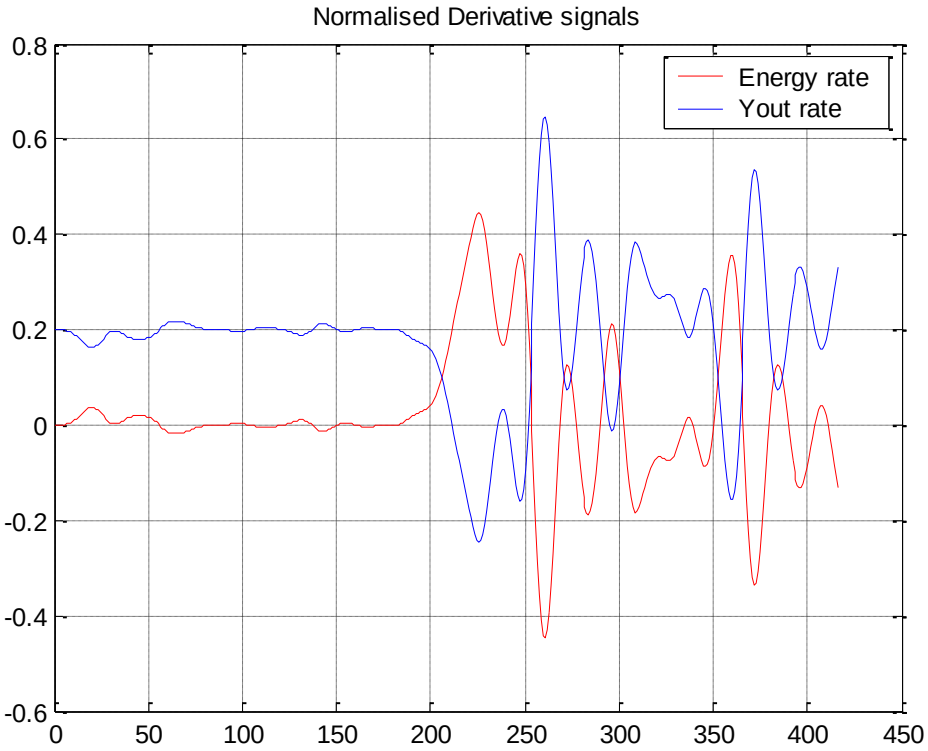

Figure-6.5b *(Amplitude-time plot) Signals before (red) and after (blue) threshold comparison in the derivative signal-path in Simulink model with* $\boldsymbol{E'_{th}}$ *= 0.2. Input is Pressure sensor signal from test rig.*

7. Conclusion and recommendations

The key findings of the literature survey and the key results of project are presented under separate headings.

7.1.1. Summary of key results of the literature survey

(a) Current methods and trends for cavitation detection were examined. Relevant patents and published papers were reviewed.

(b) Cavitation is a common problem in hydraulic systems, affecting operational efficiency and causing mechanical erosion. Its detection, prediction and resultant damage is a large area of research that has been widely studied.

(c) As cavitation phenomenon is nonstationary and highly nonlinear, its analysis, modelling and detection are very difficult. Hence traditional linear analysis and signal estimation techniques are not very useful.

(d) The direct detection of cavitation can be done only by verifying the existence of cavities, by visually observing the population of cavities in flow, which is often very difficult and impractical.

(e) Among various indirect sensing methods of cavitation detection, measuring dynamic pressure in flow and vibration monitoring in mechanical structure are more suitable for detection in jet boat.

(f) Incipient cavitation is first seen at very high frequencies and gradually spreads to low frequencies as it is fully developed.

(g) Cavity implosions induce high-frequency shock wave pressure pulses in the fluid as well as vibrations in the hydraulic structure and therefore

very fast transducers are needed.

7.1.2. Summary of key results of project

(a) Possible sensors for cavitation detection were studied and evaluated. Three types of sensors have been selected for cavitation detection- accelerometer, automotive knock sensor and pressure sensor.

(b) Tests were conducted on the Hamilton Jet test rig and on jet boat in real world conditions using the above sensors and data were analysed for cavitation signature.

(c) An automotive knock sensor or accelerometer in combination with high-frequency pressure sensor offered a better solution for cavitation detection than any vibration sensor used alone.

(d) On the boat, a knock sensor mounted on the inspection cover gave better cavitation signal than a knock sensor on the transom flange.

(e) Sensor signals were analysed for cavitation signatures in various frequency bands. It was found that cavitation characteristics were prominent in 10-15 kHz on the test rig and both 10-15 kHz and 15-20 kHz on the jet boat. For algorithm development 10-15 kHz bandwidth was chosen.

(f) A trend was observed that the signal energy initially increased at the onset of cavitation reaching a local maximum, then decreased to reach a local minimum and increased again on further increase in cavitation. This trend is previously documented by other researchers in this field and known to be of cavitation origin. Thus signal energy is taken as an estimate of cavitation intensity.

(g) The signal-energy and hence cavitation was found to increase very sharply when the static pressure in the test rig (HJ-292) is reduced more than 10 inHg vacuum (i.e. 20 inHg absolute). This was visually observed through the perspex window on the test rig. A similar increase in energy level occurred on the jet boat when engine rpm increased more than 2250 rpm.

(h) An algorithm to quantify the cavitation was developed. It was implemented in Simulink and performance was tested with the data collected from the test rig and boat.

(i) The threshold energy values used in the algorithm seem to vary with the jet unit model used. These threshold values can be easily tuned during testing of a particular jet unit model.

7.2. Conclusion and recommendations

The objective of the research is to develop an efficient, reliable, cost effective method to detect cavitation using low cost sensors and digital signal processing techniques. The following technical objectives have been achieved in relation to this objective.

1. Sensor selection

Three types of commonly available sensors have been evaluated for cavitation detection; an accelerometer, an automotive knock sensor and a pressure sensor. Cavitation data was acquired under varying conditions using a test rig at Hamilton Jet with these three types of sensors. The resulting signals have been studied and the

relative performance has been evaluated. Both the knock and accelerometer sensors were able to detect cavitation. It was found that either of these sensors in combination with a pressure sensor offered a better solution to acquire cavitation signal. The detection can be made more efficient and reliable using multiple sensors. The knock sensor provides a reasonably inexpensive and robust detection mechanism, however recent advances in sensor technology and applications may make accelerometers an attractive and cost effective option as well.

2. Detection algorithm development

A possible frequency band for the maximum detection of cavitation has been identified. An algorithm to quantify the effect of cavitation as measured by these sensors has also been developed. The algorithm uses standard digital signal processing techniques and could be reasonably implemented on production hardware. Algorithm performance has been verified using the data collected from the test-rig facility at Hamilton Jet as well as the data collected from a jet boat in real-world conditions.

The signals from the sensors are filtered and the frequency content calculated using a Fast Fourier Transform (FFT) computation. The algorithm then quantifies the amount of cavitation evident in the signal's frequency spectra using two different representations of the cavitation phenomenon; the band-limited energy contained in the signal and the rate of change of that energy. These two results can be used independently or combined as an additional input to the control scheme used to reduce cavitation or to act as a diagnostic.

As the threshold cavitation energy values used in the algorithm varies with jet unit model, it is suggested that these values be tuned at the commissioning stage of a specific jet unit model.

From the results obtained it is recommended that this project be continued to achieve the ultimate objective – a robust and cost effective cavitation detection system for production. Further works include implementation and optimising the cavitation detection algorithm in production hardware, integrating the algorithm with the control scheme of the jet boat and real-time testing of the solution.

8. References

[1] An Investigation of the Relationship Between Acoustic Emission, Vibration, Noise and Cavitation Structures on a Kaplan Turbine – Tomaž Rus, Matevž Dular, Matevž Dular, Marko Hocˇevar, Igor Kern; Transactions of the ASME, 2007

[2] Pearsall, I. S., 1966, "Acoustic Detection of Cavitation," Proc. Inst. Mech.Eng., 1-A66-67, 181, Part 3A, Paper No. 14.

[3] Cavitation monitoring and diagnosis of hydro turbine on line based on vibration and ultrasound acoustics – Su-Yi Liui, Shu-Qing Wang, Proceedings of the Sixth International Conference on Machine Learning and Cybernetics, Hong Kong, 19-22 August 2007

[4] Acoustic and vibration techniques for cavitation monitoring – P. Abbot, Atlantic applied research corporation, 1987

[5] Detection of cavitation in hydraulic turbines – Xavier Escalera et al. Mechanical Systems and Signal Processing 2004

[6] Detection of incipient cavitation in pumps using acoustic emission – G D Neill; R L Reuben; P M Sandford; E R Brown; J A Steel Proceedings of the Institution of Mechanical Engineers; 1997

[7] Detection of cavitation phenomena in centrifugal pump using audible sound – M. Cudina, Mechanical Systems and Signal Processing 2003

[8] Monitoring of the Cavitation in the Kaplan Turbine – Brane Sirok, Mako Hocevar, Igor Kern, Matej Novak, IEEE, ISIE'99

[9] Real-Time Detection of Cavitation for Hydraulic Turbomachines- Antonio Baldassarre, Maurizio De Lucia and Paolo Nesi; Real-Time Imaging

4,403–416(1998)

[10] The application of Acoustic Emission for detecting incipient cavitation and the best efficiency point of a 60KW centrifugal pump; case study – L. Alfayez, D.Mba,G.Dyson

[11] Modulation noise analyses of cavitating hydrofoils – Abbot, Philip A. (Ocean Acoustical Services and Instrumentation Systems, Inc); Arndt, Roger E.A.; Shanahan, Timothy B. Source: American Society of Mechanical Engineers, Fluids Engineering Division (Publication) FED, v 176, Bubble Noise & Cavitation Erosion in Fluid Systems, 1993, p 83-94

[12] Cavitation control for marine propulsion system; United States Patent: 5833501

[13] Control apparatus for an outboard marine engine; United States Patent: 5190487

[14] Jet propulsion boat; United States Patent: 7048598

[15] Monitoring and control of watercraft propulsion efficiency; United States Patent: 6882289

[16] Method and system for determining pump cavitation and estimating degradation in mechanical seals therefrom; United States Patent: 6487903

[17] Jet propulsion unit condition indicator; United States Patent: 5613887

[18] Research on turbine cavitation testing based on wavelet singularity detection-PU Zhong-qi, ZHANG wei, SHI Ke-ren, WU Yu-lin; Proceedings of CSEE, Vol.25.No.8 April 2005

[19] Cavitation; F. Ronald Young; Imperial College Press, 1989

[20] Cavitation and bubble dynamics; Christopher E. Brennen; Oxford University Press, 1995.

[21] Cavitation; Robert T. Knapp, James W. Daily, Frederick G. Hammitt;

McGraw-Hill, 1970

[22] On cavitation in Fluid power; Timo Koivula; Proc. of 1st FPNI-PhD Symp. Hamburg 2000, pp. 371-382

APPENDIX - TEST PLANS

Appendix-I: Test plan to acquire Cavitation data from the Test-rig

This document gives a brief description and a plan of activities to be conducted to gather cavitation data from the test-rig using knock sensor and high-frequency absolute pressure sensor.

Test system set-up:

The block diagram and a brief description of the test set-up are given below.

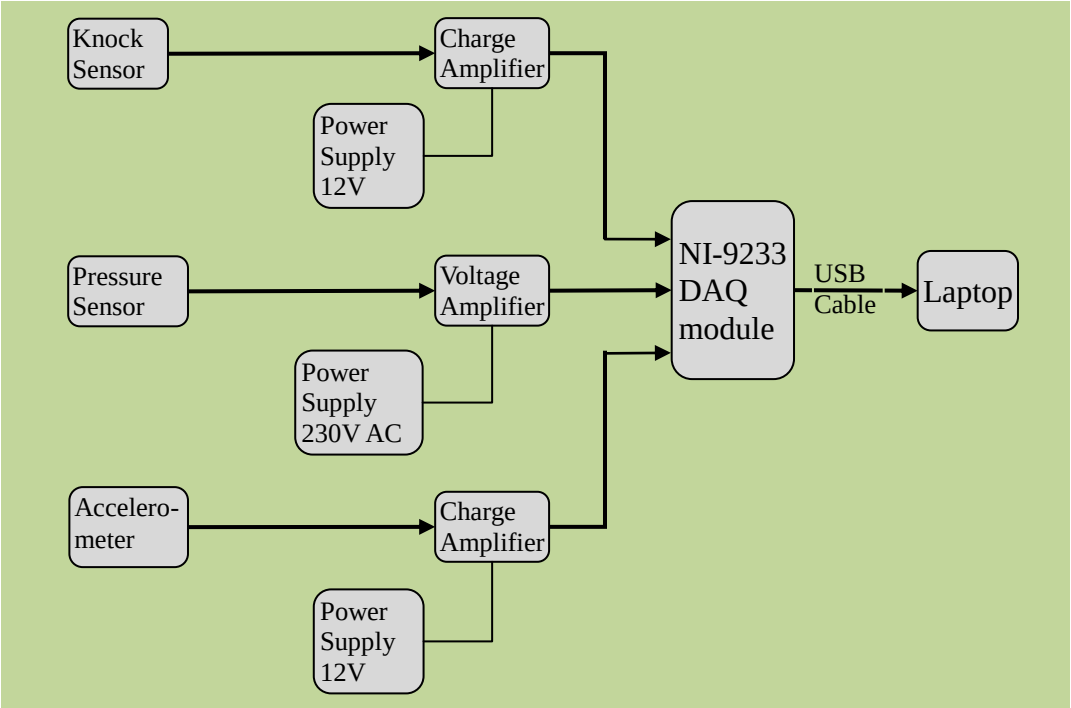

Figure-A.1 *Test-rig test instrumentation setup*

The data acquisition system used to record signals is NI-9233 C-series module from National Instrument. It can sample data simultaneously from all four channels, at a sample rate of 50 kHz. In this experiment, signals from accelerometer, knock sensor and pressure sensor are given to the Channel-0, Channel-1 and Channel-2 of the DAQ module and are recorded simultaneously at the maximum sampling rate of

50 kHz. The sampled signal is recorded real-time in a laptop using the DAQ software, *Signal Express* from National Instruments.

Test instrument & component specifications:

Knock sensor and charge-amplifier system:

Knock sensor	: Bosch knock sensor KS-R
Frequency range	: 1 kHz – 20 kHz
Knock sensor Sensitivity at 5 KHz	: 26mV/g
Charge-amplifier gain	: 200
Charge-amplifier maximum output voltage	: 5V
Charge-amplifier power supply	: 12V DC

Pressure sensor and amplifier system:

Pressure sensor	: Kistler 4075A10
Pressure range	: 0...10 bar (Absolute)
Natural frequency	: > 45 kHz
Sensitivity	: 50 mV/bar
Amplifier output range	: 0...10 V
Amplifier frequency range	: > 60 kHz (measured)

Note: - The amplifier was obtained from the UoC mechanical department which was custom made at the university to be used with the Kistler 4075A10. No other technical spec. of the amplifier was available.

Accelerometer and amplifier system

Accelerometer	: B&K type 4333
Voltage sensitivity	: 17.8 mV/g
Charge sensitivity	: 19.3 pC/g
Undamped natural frequency	: 60 kHz

Charge amplifier type : B&K Type 2624

Data acquisition module (NI-9233):

Sampling Frequency : 50 kS/sec

DAQ ADC type : Sigma-Delta (with analog pre-filtering)

Resolution : 24 bits

IEPE excitation current : 2.2 mA (typical)

Input signal max. Voltage : 5 V

Idle channel noise (at 50 kS/sec) : 95 dBFS

Test Plan:

The following tests are conducted on the test-rig to record cavitation signals.

Group-1 Data: Low rpm

Data is recorded for different pressures keeping the RPM constant

Sl. No.	Test-rig pressure	Data recorded
1	14 psi	RPM = 1350
2	9 psi	
3	5 psi	
4	0 psi	
5	- 6	
6	- 8	
7	- 10	
8	- 12	
9	- 15	

Group-2 Data : High rpm

Data is recorded for different pressures keeping the RPM constant

Sl. No.	Test-rig pressure	Data recorded
1	14 psi	RPM = 1760
2	10 psi	
3	5 psi	
4	0 psi	
5	- 8	
6	- 15	
7	- 16	
8	- 18	

Group-3 Data: Transient pressure test (Low rpm)

Group-3 test and Group-12 test are identical.

Group-4 Data : Transient data pressure test (medium rpm)

Group-4 test and Group-13 test are identical.

Group-5 Data : Transient data pressure test (medium rpm)

Group-5 test and Group-14 test are identical.

Group-6 Data: Constant pressure, different rpm (steady-state)

Pressure in the test-rig is held constant. Data was collected at different steady-state rpm.

Sl. No.	Test-rig RPM	Data recorded
1	1450	Pressure = 5 psi
2	1500	
3	1550	
4	1600	
5	1650	
6	1700	
7	1760	

Group-7 Data: Constant pressure, different rpm (steady-state)

Pressure in the test-rig is held constant. Data was collected at different steady-state rpm.

Sl. No.	Test-rig RPM	Data recorded
1	1450	Pressure = 0 psi
2	1500	
3	1550	
4	1600	
5	1650	
6	1700	
7	1760	

Group-8 Data: Constant pressure, different rpm (steady-state)

Pressure in the test-rig is held constant. Data was collected at different steady-state rpm.

Sl. No.	Test-rig RPM	Data recorded
1	1450	Pressure = -10
2	1500	
3	1550	
4	1600	
5	1650	
6	1700	
7	1760	

Group-9 Data: Constant pressure, transient rpm

Impeller RPM in increased in stepwise from 1350 to 1760 rpm, at a constant pressure.

Sl. No.	RPM Range	Data recorded
1	1350 – 1760 rpm	Pressure = 5 psi

Group-10 Data: Constant pressure, transient rpm

Impeller RPM in increased in stepwise from 1350 to 1760 rpm, at a constant pressure.

Sl. No.	RPM Range	Data recorded
1	1350 – 1760 rpm	Pressure = 0 psi

Group-11 Data: Constant pressure, transient rpm

Impeller RPM in increased in stepwise from 1350 to 1760 rpm, at a constant pressure.

Sl. No.	RPM Range	Data recorded
1	1350 – 1760 rpm	Pressure = - 10

Group-12 Data: Constant RPM, transient pressure with shaft power variation recorded

Pressure in the test-rig was decreased by opening the valve, allowing the water to drain. RPM is held constant. The shaft power variation is recorded on the test-rig PC.

Sl. No.	RPM Range	Data recorded
1	14 psi - -18	RPM = 1200 (Recorded as ***Gr10_power_1200*** in Labview SignalExpress)

Group-13 Data: Constant RPM, transient pressure with shaft power variation recorded

Pressure in the test-rig was decreased by opening the valve, allowing the water to drain. RPM is held constant. The shaft power variation is recorded on the test-rig PC.

Sl. No.	RPM Range	Data recorded
1	14 psi - -18	RPM = 1500 (Recorded as ***Gr10_power_1500*** in Labview SignalExpress)

Group-14 Data: Constant RPM, transient pressure with shaft power variation recorded

Pressure in the test-rig was decreased by opening the valve, allowing the water to drain. RPM is held constant. The shaft power variation is recorded on the test-rig PC.

Sl. No.	RPM Range	Data recorded
1	14 psi - -18	RPM = 1760 (Recorded as ***Gr10_power_1760_repeat*** in Labview SignalExpress)

Appendix-II: Test plan to acquire Cavitation data from the jet boat

This document gives a brief description and a plan of activities to be conducted to gather cavitation data from the jet boat in real-world conditions.

Test system set-up:

The block diagram and a brief description of the test set-up are given below.

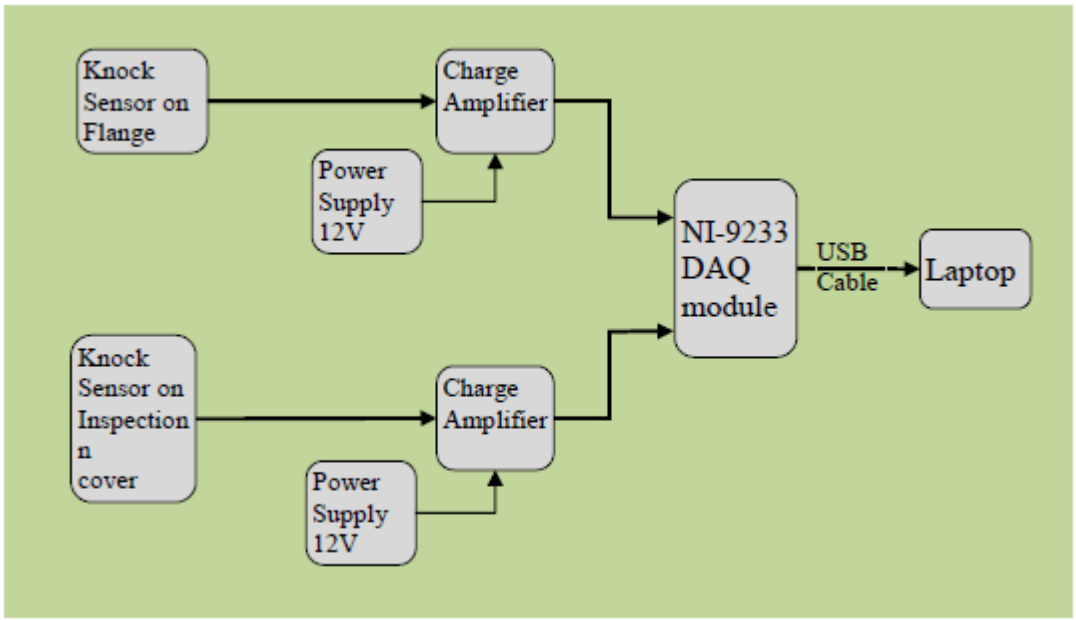

Figure-A.2 *Boat test instrumentation setup*

This experiment is designed to collect cavitation related data and to analyse it to understand the effect of external variables has in successfully detecting cavitation in a jet unit, in real-world conditions. Although the boat has two jet units, only one jet unit is used in the experiment in order to avoid the effects of possible noise that may be induced to the measurement due to the operation of a second jet engine. The jet unit model used to acquire data is HJ-213.

The vibration sensor used to gather cavitation signals is the Bosch piezoelectric knock sensor (KS-R). This is the same knock sensor used to collect data from the test-rig earlier. The signal from the knock sensor is further conditioned by a charge amplifier before it is fed to the data acquisition module. A 12V DC voltage source is used to supply power to the charge amplifier, which is designed to accept voltage in the range of 10-20V.

As the vibration signal characteristics are very much depended on the engine rpm, the engine-rev. information is also recorded, which is produced by the RPM-sensor in the boat. The RPM sensor signal is directly fed to the second channel of the DAQ system.

The data acquisition system used to record signals is NI-9233 C-series module from National Instrument. It can sample data simultaneously from all four channels, at a sample rate of

50 kHz. In this experiment, signals from the knock sensor and the RPM sensor are given to the Channel-0 and Channel-1 of the DAQ module and are recorded simultaneously at the maximum sampling rate of 50 kHz.

The sampled signal is recorded real-time in a laptop using the DAQ software, *Signal Express* from National Instruments.

Test instrument & component specifications:

Knock sensor and charge-amplifier system:

Knock sensor : Bosch knock sensor KS-R

Frequency range : 1 kHz – 20 kHz

Knock sensor Sensitivity at 5 KHz : 26mV/g

Charge-amplifier gain : 200

Charge-amplifier maximum output voltage : 5V

Charge-amplifier power supply : 12V DC

Data acquisition module (NI-9233):

Sampling Frequency : 50 kS/sec

DAQ ADC type : Sigma-Delta (with analog pre-filtering)

Resolution : 24 bits

IEPE excitation current : 2.2 mA (typical)

Input signal max. Voltage : 5 V

Idle channel noise (at 50 kS/sec) : 95 dBFS

RPM sensor:

RPM information is obtained from the onboard RPM sensor in the boat.

Other components:

USB Active extension cable length (between NI-9233 and laptop) : 5 metre

USB extension cable current rating : 100 mA for 5 metre

Test Plan:

The following tests are conducted to record cavitation signals.

Note: Only one jet unit is used throughout the experiment

Group-1 Data: (Boat stationary)

Data is recorded for different RPM, keeping the ***boat stationary*** with reverse bucket held at zero-speed position.

Sl. No.	Engine RPM	Data recorded
1	1000	
2	1250	
3	1500	
4	1750	
5	2000	
6	2250	
7	2500	
8	2750	
9	3000	
10	3250	
11	3500	
12	3800	

Group-2 Data : Transient data (Initially boat stationary)

Data is recorded for each RPM range, keeping the ***boat stationary***, increase RPM from *idle rpm* to a predetermined value.

Sl.No	Engine RPM range	Data recorded
1	750 – 1500 (turbo charger cut-in rev.)	
2	1500 – 3800	
3	750 – 1500	
4	1500 – 3800	

*Group-3 Data: (Boat moving at a speed of **5 knots**)*

The data is recorded at different rpm with the boat moving slowly at a **constant speed of 5 knots**

Sl. No.	Engine RPM	Data recorded
1	1000	
2	1250	
3	1500	
4	1750	
5	2000	
6	2250	
7	2500	
8	2750	
9	3000	
10	3250	
11	3500	
12	3800	

Group-4 Data : Transient data (Initially boat moving at 5 knots) (OPTIONAL)

Data is recorded for each RPM range, keeping the ***boat moving*** at a ***constant speed*** of ***5 knots*** (also by adjusting the bucket position to maintain the speed), increase RPM from *idle rpm* to a predetermined value.

Sl.No	Engine RPM range	Data recorded
1	750 – 1500 (turbo charger cut-in rev.)	
2	1500 – 3800	
3	750 – 1500	
4	1500 – 3800	

Group-5 Data: (Boat moving)

RPM is held high (greater than 2500) and held constant with jet unit cavitating significantly. The reverse bucket is raised, *allowing the boat to move at constant speed* and data is recorded.

Sl. No.	Boat speed (Knot)	Data recorded
1	0	
2	2	
3	4	
4	6	
5	8	
6	10	
7	12	
8	14	
9	16	

Group-6 Data: Transient data (Boat moving)

Initially ***the boat is held stationary at idle rpm*** and the rpm is increased rapidly to a predetermined value, *allowing the boat to accelerate*.

Sl. No	Engine RPM range	Data recorded
1	750 - 3800	
2	750 - 3800	